CHAPTER 4

RESULT AND DISCUSSION

4.1 Property and Characteristic of Raw Materials

4.1.1 Sand Properties

A variety of sands (foundry sands) are used in casting processes. Each sand differs in composition, grain size and distribution, purity shape, etc. These properties are key factors in successful moldmaking and coremaking and in subsequent reclamation processes. Sand testing is used to determine and characterise these properties, so that fit for purpose molds and cores can be produced thus preventing casting defects.

Three sands were used in the present study. Australian sand is suitable for use in shell coremaking because it has rounded grains, and gives high permeability. It also has a fine particle size producing castings with a good surface finish. In addition, Australian sand has a low surface area and hence requires the least amount of resin for bonding. One disadvantage is that this sand is more expensive than local sands.

Rayong sand is suitable for production of Shell molds because the size, size distribution, and shape of the sand grains allow good control of permeability. In addition, this sand has a low expansion coefficient.

Reclaimed sand is used in foundries to reduce costs and problems with the control of environmentally undesirable contaminants in the discarded sand. The properties of reclaimed sand are such that it is normally used for Shell molds.

Analytical results on chemical and physical properties of three sands are summarized in Table 4.1 and 4.2, respectively.

Table 4.1 Chemical composition and properties of sands

Chemical composition and properties	Rayong sand	Australian sand	Reclaimed sand
Moisture, %	0.09	0.22	0.10
Loss on ignition, %	0.41	0.73	0.21
Silica (SiO_2),%	90.2	96.3	93.1
Alumina (Al_2O_3),%	4.80	1.07	3.42
Iron oxide (Fe_2O_3),%	0.40	0.25	0.44
Titanium dioxide (TiO_2),%	0.70	0.07	0.10
Calcium oxide (CaO),%	0.13	0.75	0.27
Magnesium oxide (MgO),%	0.06	None	0.08
Sodium oxide (Na_2O),%	0.32	0.12	0.40
Potassium oxide (K_2O),%	3.32	0.48	1.60
Acid demand value (ADV)	6.1	35	12.8
pH	8.6	9.2	9.8

Table 4.2 Physical properties of sands

Physical properties	Rayong sand	Australian sand	Reclaimed sand
Specific gravity	2.51	2.53	2.51
AFS grain fineness number	53.6	58.6	51.4
Dry density, gm/cc	1.64	1.60	1.62
Surface area, cm^2/gm	111	102	110
Coefficient of angularity	1.18	0.97	1.22
Color	Brownish	Light brown	Dark brown

From Table 4.1, it is seen that Australian sand has the highest silica content. This value indicates that Australian sand has high refractoriness but suffers from the highest coefficient of thermal expansion (as seen in Figure 4.1) because silica undergoes a phase change from alpha to beta quartz at $573^{\circ}C$ resulting in a volume expansion. Rayong sand contains 3.32% of potassium oxide (K_2O) which reduces refractoriness and can result in burn-on problems. Ideally sand should contain no more than 0.5% potassium oxide. All sands contain less than 1% of calcium and magnesium oxide less than 1%.

In addition, acid demand value (ADV), moisture content, loss on ignition (LOI), pH values of sand are basic information that should be known. These values are also important to assess the surface contamination of the sands.

The ADV of sand is measured by titration of the acid requirements of sand. It is expressed as the number of milliequivalents of 0.1N HCl which is used or reacted with the
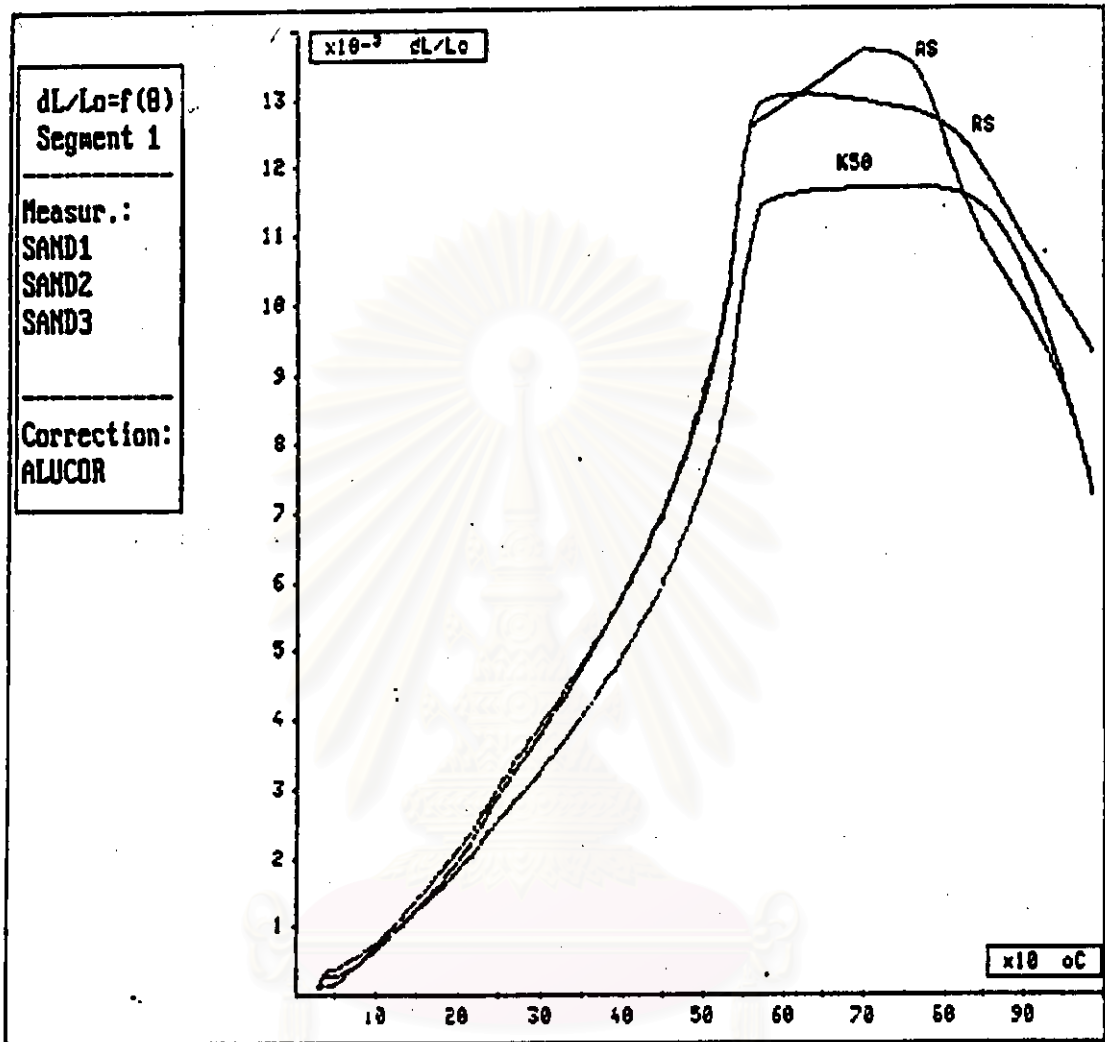
Figure 4.1 Temperature-expansion curves for three sands

Note: AS represents an Australian sand

RS represents a reclaimed sand

K 50 represents a Rayong sand

sand being tested. The acid demand test provides information on the degree of alkaline contaminants in the sand. It has an important influence on the catalyst requirement where acid catalysts are used as in Furan processes. The ADV of a Rayong sand reclaimed sand and Australian sand had ADV of 6.1, 12.8 and 35, respectively. It has been shown that sand surface chemistry had alkaline contaminants. Therefore, these sands are suitable for the Shell Process because hexamine is a basic catalyst.

The pH value of sand is measured by adding the sand to distilled water and measuring the hydrogen ion concentration of the water layer. This value shows level of soluble acidic or alkaline contamination. The pH value of Rayong sand, reclaimed sand and Australian sand were 8.6, 9.2, and 9.8, respectively. These numbers indicate soluble alkaline contaminants on sand surface.

Loss on ignition shows the level of organic contaminants and this test is used in assessing the residue of resin binder in reclaimed sand. This residue resin can influence re-bond strengths and casting performance. The LOI of three sands had low values, which show a small amount of organic contaminants, thereby, little difference is expected between the bonding system for new sands and the re-bonding for reclaimed sand.

The physical properties results of three sands were reported in Table 4.2. The AFS grain fineness number of reclaimed sand, Rayong sand, and Australian sand are 51.4, 53.6, and 58.6, respectively. These values can be used to indicate the approximately average grain size of these sands. AFS fineness number is replaced by ISO metric sieves which enable average grain size to be calculated in μm. Approximate the relationships are sieve number $50 \approx 280$ μm and sieve mesh number $60 \approx 250$ μm. Thus, the average grain size

of reclaimed sand, Rayong sand, and Australian sand can be indicated the approximately 280, 275 , and 250 μm, respectively.

Table 4.3 Percentage of retained sand on various sieve number of three sands

USA sieve number	Rayong sand weight retained on sieve,%	Australian sand weight retained on sieve,%	Reclaimed sand weight retained on sieve%
20	0.01	-	0.02
30	0.01	-	0.03
40	9.54	-	9.34
50	26.1	1.87	28.8
70	40.8	58.1	42.4
100	14.2	38.4	12.7
140	7.7	1.23	5.69
200	1.59	0.11	0.7
270	0.04	0.05	0.04
pan	0.01	0.15	0.01
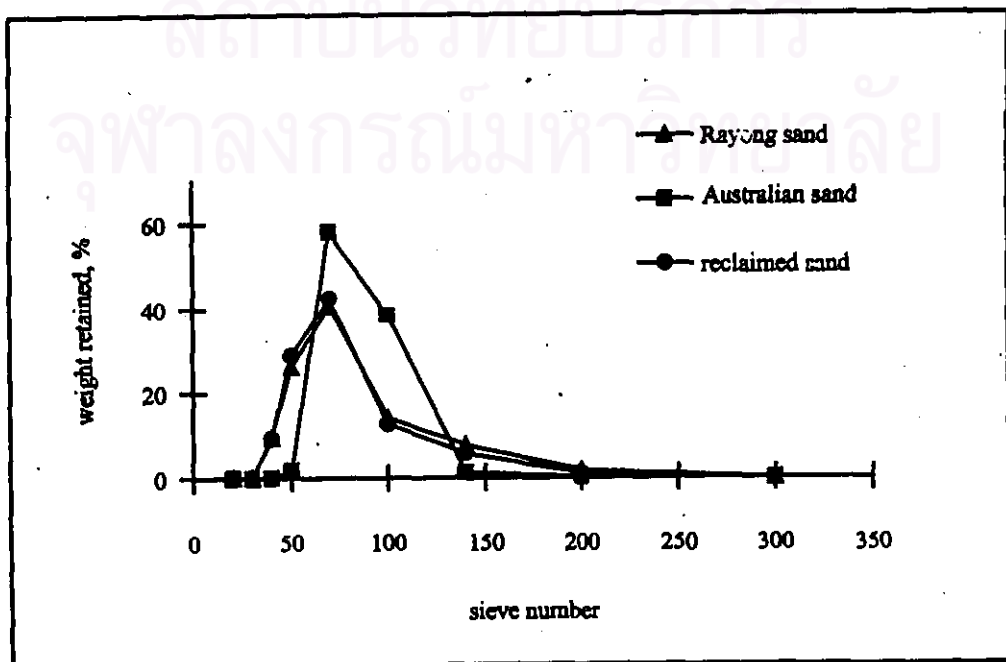
Figure 4.2 AFS grain distribution of sands

Table 4.3 was demonstrated the sieve analysis of three sands. It has been shown that the size distribution of Rayong sand was similar to reclaimed sand, as shown in Figure 4.2. The characteristics of two sands consist of coarse and fine particles. Lemon (1993) reported that that the best size distribution within sand is a reasonable amount of grains spread over four or five sieves. This appears to give the highest strengths on compaction and maximum resistance to expansion defects because voids between coarser particles were packed with finer particles give maximum compaction/density and minimum permeability. For Australian sand has smaller size. Therefore, size distribution of Australian sand is narrow because of the size of sand grains do not differ, as illustrated in Figure 4.2.

In addition, surface area and coefficient of angularity can lead to predict the shape of sand grains. Rayong sand and reclaimed sand have round/sub-angular grains giving these sands a high surface area and a coefficient of angularity $\approx$ 1.18-1.22. Australian sand has round grains giving this sand a low surface area and a coefficient of angularity $\approx$ 0.97. Therefore, Australian sand is preferred for making cores because it requires the smallest amounts of resin and it has very good flowability.

The angularity of sand can be estimated by visual examination with a low power optical microscope (35x), as shown in Figure 4.3-4.5.
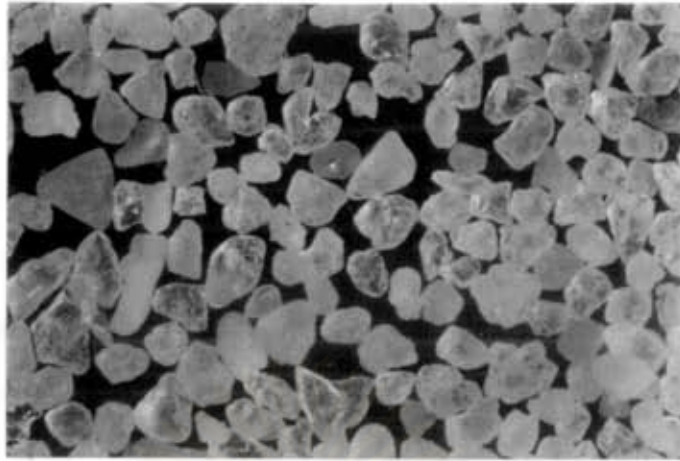
Figure 4.3 Optical microscopic examination (35x) of the grain shapes of Australian sand
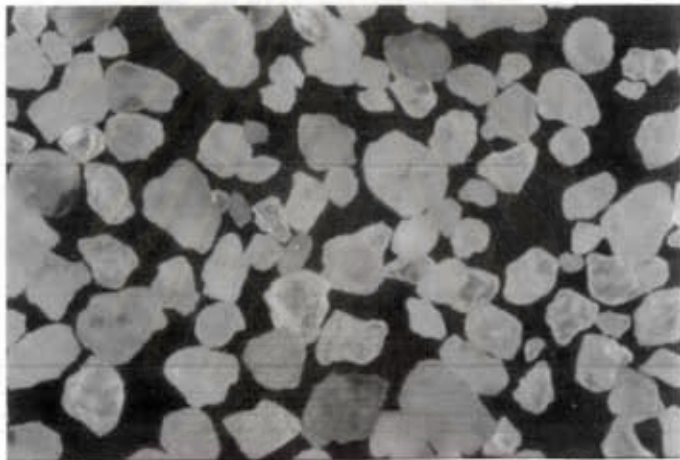

Figure 4.4 Optical microscopic examination (35x) of the grain shapes of Rayong sand
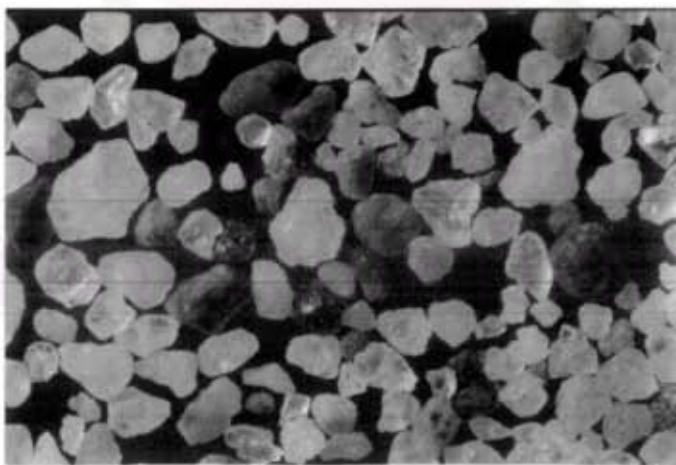

Figure 4.5 Optical microscopic examination (35x) of the grain shapes of reclaimed sand

4.1.2 Resins Properties

This section presents and discusses results from the characterization of Thai and imported resins. Techniques applied to study structure and properties of these resins include ^{13}C-NMR spectroscopy, Gel Permeation Chromatography (GPC), Differential Scanning Calorimetry (DSC), Thermogravimetric Analysis(TGA), and melting point measurement.

Data presented in this section provides information on resin structure features and properties, factors that are crucial in understanding and predicting novolac resins' behaviors, especially in use as a binder in shell molding. This information includes structure resin isomers, resin thermal and physical properties, and the influence of structure on resin flowability and gelation.

Characterization results of Thai and imported novolac resins are summerized in Table 4.4

Table 4.4 Properties of Thai resin and imported resins

Properties	Thai resin (FD-1)	Imported resin (PSM-6412)
Appearance	granular	Granular
Color	Black brown	Light orange
^{13}C-NMR analysis		
o,o',% (methylene bridges)	27	61
o,p',% (methylene bridges)	49	26
p,p',% (methylene bridges)	24	13
GPC analysis		
M_n	876	749
M_w	3226	3056
Polydispersity	3.68	4.08
*Endothermic transition range , $^{\circ}$C	82-88	70-82
**melting point , $^{\circ}$C	91	82
***Gelation time, sec/150,$^{\circ}$C	44	61
***Flow, mm/125,$^{\circ}$C	37	48

Note: * determined by DSC and ** determined by melting point measurement

*** given by suppliers

4.1.2.1 Structure Analysis

^{13}C Nuclear Magnetic Resonance (NMR) is a powerful tool and direct method for obtaining structural information of polymers, configuration, geometrical isomerization, to quantify chain branching, to assess conformational preference and flexibility. The

chemical shift is recorded which respresents the signals of slightly different frequencies for each chemically different nucleus, depending on its chemical binding and position in a molecule. This variation is caused by the cloud of electrons about each nucleus, which shields the nucleus against the magnetic field. This variation is termed chemical shifts and is commonly expressed in relation to the resonance of tetramethylsilane (TMS) as the zero reference.

The spectra of Thai and imported resins are reported in Figure 4.6 and 4.7, respectively. These spectra can be split into five main areas:

1. The chemical shifts of phenoxy carbon (C_1-OH) are between 153.8 and 156.2 ppm. The C_1 signals of phenolic rings, in which the reaction has taken place at *ortho* position have lower chemical shift values than the ones reacted to *para* positions.

2. The free *meta* and substitution with a methyl group ($-CH_2OH$) causes a downfield shift of the *ortho* and *para* carbon resonance from 128.4 to 134.2 ppm.

3. The free *ortho* and *para* carbon occur at 115.9-116.0 ppm and 120.5 ppm, respectively.

4. The methanol could be observed at 48.1-49.8 ppm.

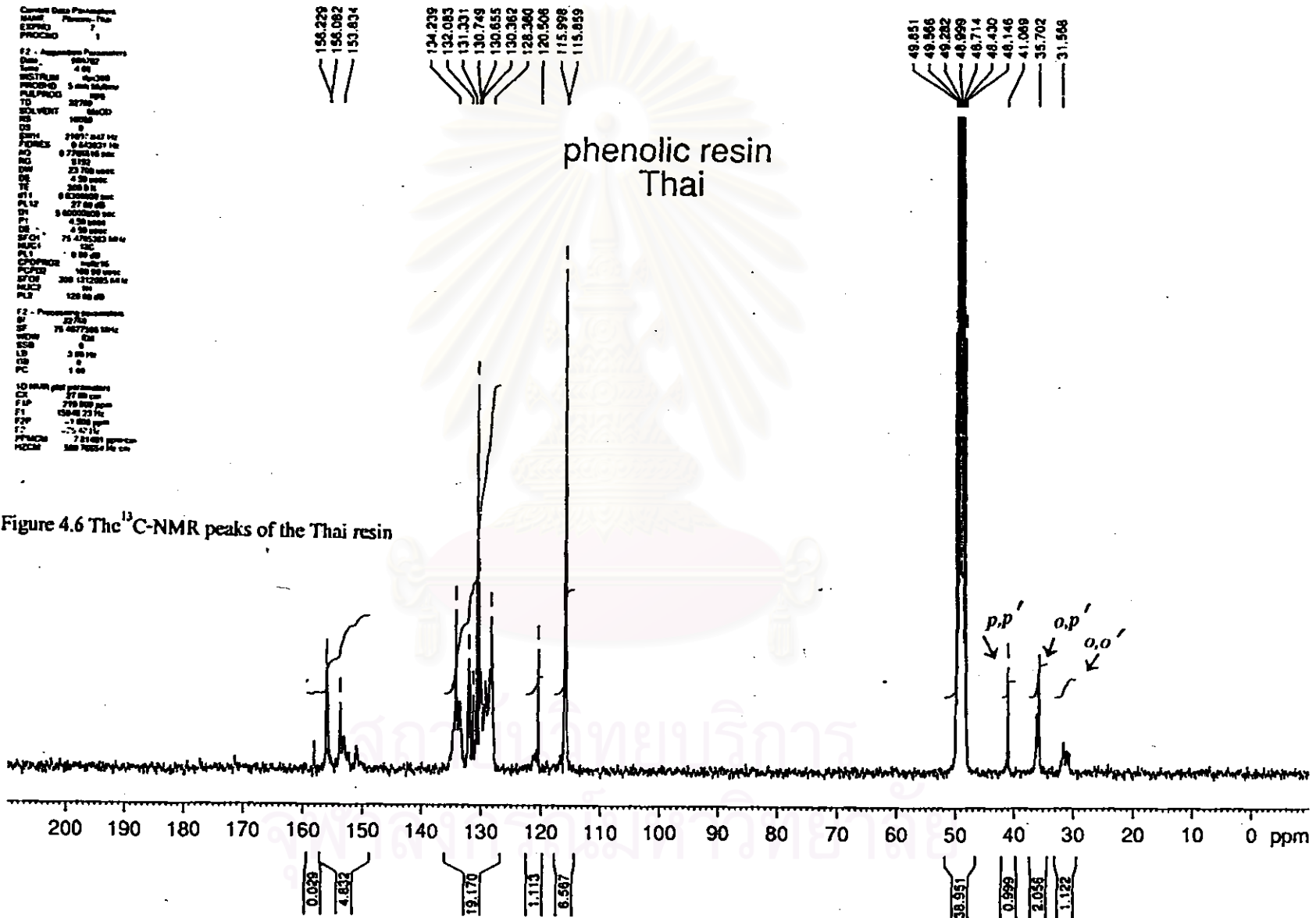5. The methylene bridges ($-CH_2-$) group have signals from 30.6 to 41.1 ppm.

Figure 4.6 The ^{13}C-NMR peaks of the Thai resin

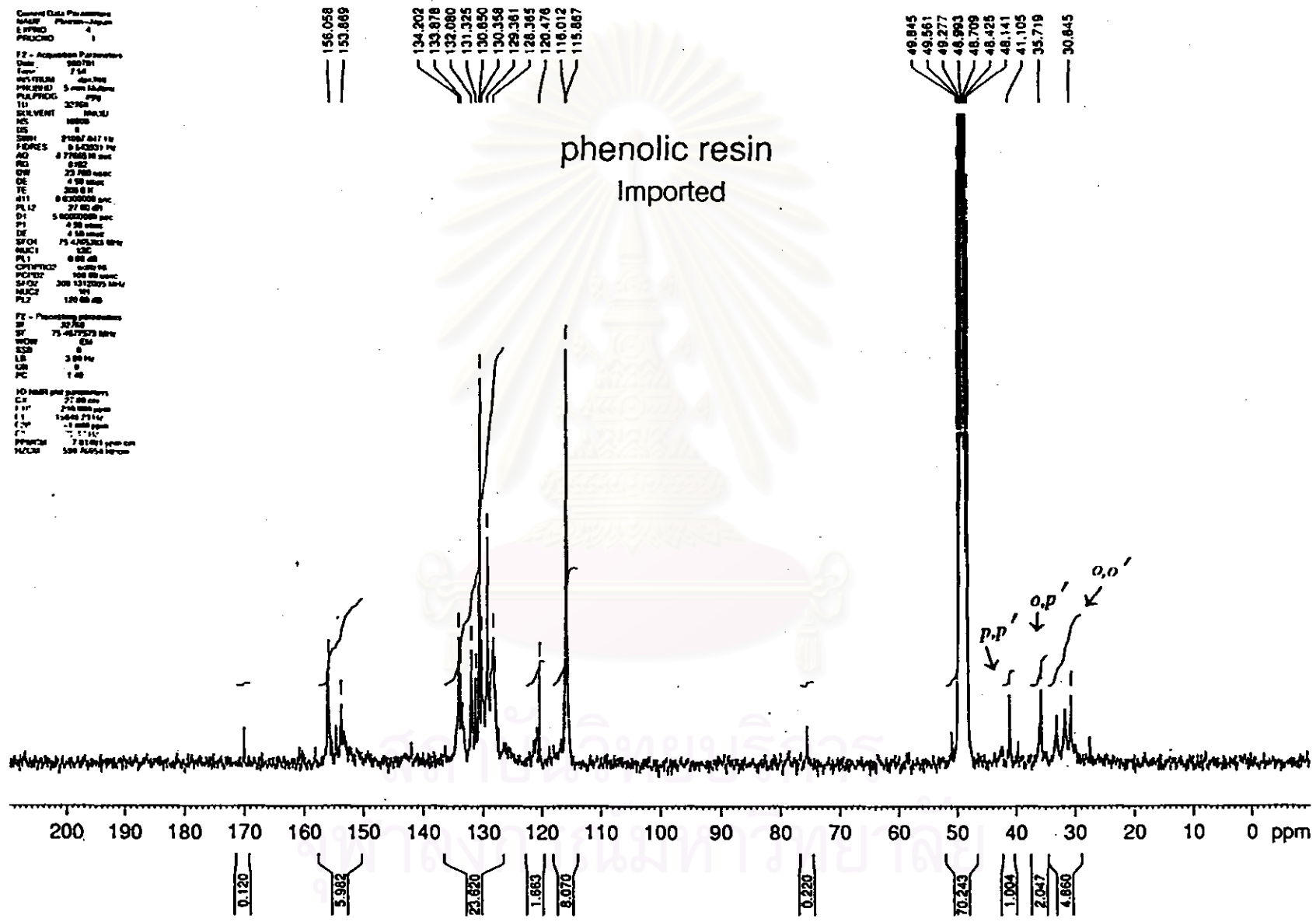Figure 4.6 The ^{13}C-NMR peaks of Thai resin

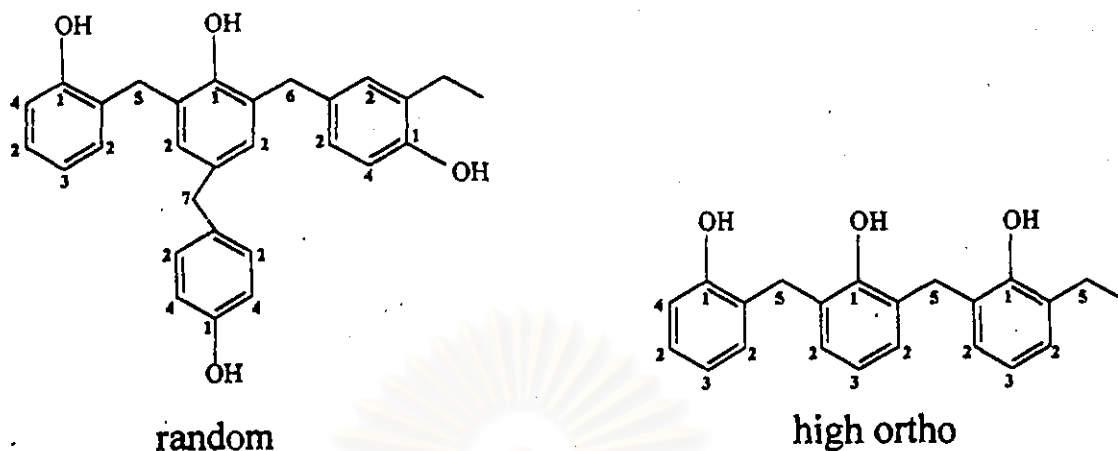**Figure 4.7 The ^{13}C-NMR peaks of imported resin**

Figure 4.8 Structure of random and high ortho links of phenolic novolac resin

Table 4.5 The specific ^{13}C-NMR peaks of the phenolic resins

Carbon region (as shown in above Figure 4.8	Functional group	Relation position	Chemical shift (shift)
1	Phenoxy ring		150.40-157.50
	Phenoxy, alkylated in ortho position		154.80-156.10
	Phenoxy, alkylated in para position		156.50-156.80
2	meta free positions on the phenolic ring		124.66-133.50
3	para free positions on the phenolic ring		119.20-119.50
4	meta free positions on the phenolic ring		114.70-115.10
5	Ph-CH$_2$-Ph	Ortho-ortho	29.21-31.40
		Ortho-para	34.27-36.0
		Para-para	40.83-41.0

^{13}C Nuclear Magnetic Resonance (NMR) spectroscopy was used to study structure of novolac resin. ^{13}C NMR has proven to be a powerful tool in the identification of resin isomers. This technique gives signals for all nonequivalent carbon atoms at different chemical shifts. Data obtained can be used to identify different functional groups or structural isomers. For instance, the carbon atoms of the methylene bridge are in different environments depending on whether the methylene is ortho or para to the phenolic hydroxyl groups. The characterisitc peaks used for interpretation of the NMR results of phenolic resins are summarized in Table 4.5. The data was obtained from the studies by Pizzi and Panamgama (1995), and Halopaimen *et al* (1997).

From Figures 4.6 and 4.7, comparing the characteristic peaks of ortho-ortho (*o,o*), ortho-para (*o,p*), and para-para (*p,p*) methylene bridge of Thai with imported resins, it can be clearly seen that the area under the peaks at corresponding chemical shifts of 31.5, 35.7, and 41.0 ppm of the two resins are dramatically different. Such three isomer peaks of *o,o*, *o,p*, *p,p* are indicated by arrows in the Figures, and numbers specified under the lines represent areas of the peaks at certain chemical shifts. Peak areas were measured by integration to give a ratio of three isomers of resins. In Figure 4.6, the integrated peak area at 31.5, 35.7, and 41.0 ppm are 1.122, 2.056, and 0.999. These results give a ratio of the three isomers of the Thai novolac resin to be 27, 49, and 24 %. It is, therefore, very likely that this Thai resin should consist of phenol rings randomly linked with *ortho-ortho, ortho-para,* and *para-para* methylene bridges. In the case of imported resin, the integrated peak areas at 30.6, 35.7, and 41.1 ppm are 4.860, 2.047, and 1.004, respectively, see Figure 4.7. These results also give the proportion of *ortho-ortho, ortho-para,* and *para-para* methylene bridges of imported resin as 61, 26, and 13 % respectively. Obtained data suggest a great tendency of having high-ortho links of phenol rings in imported novolac resin.

Koft (1988) described that novolac resins (two-stage type as used in this study) are prepared with acid catalyst. A normal ratio of the three isomers for an acid-catalyzed novolac is 18:50:30 (o,o' : o,p' : p,p'). This reported isomer ratio is not much different from that of Thai resins, but shows a large difference as compared to the resulting ratio for imported resin. In order to better understand such findings, it is worthwhile looking at factors influencing resin structures. Resin structure can be controlled by the catalyst, pH (acid range), and phenol to formaldehyde ratio (Bender and Farnham, 1949). With regard to pH of the reaction in the acid range, the p,p' isomer is favored by increasing acidity, with greatest yields at the lowest pH (0) (Finn and Musty, 1950). The o,p' isomer has a maximum yield at a pH of ≈ 0.75 and decreasing yields at lower and higher pH. When the pH range from 4 to 7 with specific metal catalysts (e.g., oxides of zinc, aluminium, and magnesium), the preparation of o,o' isomer is favorable. Previous studies have also revealed that hydroxides of transition metal catalysts such as cobalt and copper will also promote the formation of o,o' isomer (Peer, 1960). Furthermores, in the intermediate pH of 4-7, a 15-30% molar excess of phenol over the formaldehyde also aids in directing the o,o' structure of novolac resins.

Different structures or isomers between Thai and imported resins as indicated by dissimilar ratios of o,o' : o,p' : p,p' can affect curing behavior, flowability as well as reactivity of the resins. It has been reported that the reactivity of the o,o' isomers is superior to the p,p' isomers. For instance, gel time of novolac resins with 15% hexamine at 160°C of o,o', o,p', and p,p' are 60, 240, and 175 seconds, respectively. High cure rate of high ortho novolacs with hexamine can be attributed to the o,o' structure effects. As seen in chemical equation (7), the close proximity of ring hydroxyl groups to each other provides an opportunity for hydrogen binding (Koft, 1988). In addition to hydrogen bonding, the ortho novolacs readily release hydrogen ion which has "hyperacid" property.

Such hyperacidity may help promote the decomposition of hexamine, and in turn the reactivity of o,o' resin. However, the clear picture of how hyperacidity affects the enhanced cure rate has not yet understood.

In the case of Thai novolacs consisting of three isomers (o,o', o,p', and p,p') and with no high o,o' proportion, the resin structure could be the formation of complex mixtures of random ortho-ortho, ortho-para, and para-para methylene linkages and posses branching. A schematic of this branch structure is presented in Figure 4.8. It is known that the branching resin has a higher content of end groups and cure faster because of the higher resin functionality. (Koft, 1988). This structure effect can, then, explain why the gelation time of Thai resin is shorter than that of the high. o,o' imported resin.

$$(7)$$
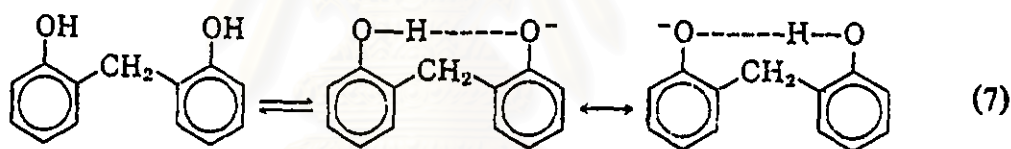
4.1.2.2 Curing and Flow Properties

Cure rate or gelation time and flow properties are important characteristics of resin used as binder in many applications as well as in shell molding. Cure rate is the speed with which a phenolic resin reaches a commercially useful degree of crosslinking. Cure rate can be simply approximated by gel time. Cure rate or gel time are affected by the temperature, pH, resin structure ,moisture , free phenol, and hexamine content.

The effect of resin structure on cure has been discussed in connection with the faster gelation time (44 sec) of Thai resin than imported resin (61 sec). This may be

attributed to a more highly branching chains and more functionality in Thai resin which greatly enhance cross-linking or gelation.

In the case of flow properties, the flow length is a function of both the curing rate and the melt viscosity. If the curing rate and melt viscosity are high, the flow length will be reduced. The short flow length resins (as observed in Thai resin) have a tendency to harden before they have time to form a strong bond between sand grains. For the low melt viscosity resin or high flow length (as observed in imported resin), the long flow length resins can produce higher tensile strength bonds. However, it should be noted that if the melt viscosity is too low, this may contribute to peelback in the shell molds and cores. The medium flow length resins have a wide range of application and are a good compromise between strength and peelback tendency. It can be seen that the flowability and cure rate of resins are crucial factors influencing the bond strength properties in resin coated sand.

4.1.2.3 Molecular Weight Measurement

Gel Permeation Chromatography (GPC) was used to determine average molecular weight (M_w, and M_n), molecular weight distribution, and polydispersity index (M_w/M_n). In this analysis, average molecular weight of uncured novolac (low molecular weight materials) of Thai and imported resins were measured and reported in Table 4.4.

Since the resins of interest in this study are heterogeneous polymers. It appears that M_w are greater than the M_n, and degree of difference between the two values (M_w/M_n) is a measure of breath or molecular weight distribution. It should be noted that the uncured resin contains a great number of small molecules in a given weight, therefore, the M_n is

influenced more by the low molecular weight species whereas the M_w reflects the higher molecular weight molecules. However, This section discusses on M_n of the Thai and imported resins as to compare the resulting values with the usually reported M_n of commercial novolac resins.

Average molecular weights (M_n) of Thai and imported resins are approximately 876 and 749, respectively. These two values are in the range of commercial practice M_n valves of novolac resins ($\approx$ 500 to over 900). The observed average molecular weight of novolac resins can determine its melting point or viscosity and processing properties. In general, melt viscosity of the resin increases with molecular weight (Jones, 1952). Based on the higher M_n of Thai resin, this implies a tendency of Thai resin being more viscous than the imported resin. However, several factors can affect molecular weight of phenolic resin. These include the ratio of phenol to formaldehyde, the type of catalyst (acid or alkaline), and the time and temperature of reaction.

4.1.2.4 Thermal Properties

4.1.2.4.1 Thermogravimetric Analysis (TGA)

Thermogravimetric Analysis and Differential Scanning Calorimeter are two thermal analysis techniques applied to study phenolic resins. Thermal stability, compositional analysis, and decomposition study were carried out by TGA. The thermogram of Thai and imported resins are shown in the Appendices, Figure B-1. It has been found that Thai resin is considerably more stable than imported resin as evidenced by its higher decomposition temperature of $\approx$ 428°C as compared to that of imported resin of

$\approx 380^{\circ}$C. Another important observation is that at the same temperature weight loss of a Thai resin was slower than that for the imported resin. Major weight loss of the resin takes place during the temperature period of up to 400°C. Above 440°C, char formation occurs (Nakamura and Atlas, 1960). It is known that phenolic resins give a residue on combustion. This residue may be high temperature resistant additives or some inorganic substances in the resin. The residue content can be determined from weight % of the sample at that high temperature (i.e., $\approx 800^{\circ}$C in this analysis). As shown in Figure B-1 TGA results revealed that the residue content of Thai resin and imported resin were approximately 30% and 18%, respectively. This result is indicative of major difference in composition of the two resins. Note that residual binder and inorganic substances may also have a direct effect on reclaimed sand characteristics and eventually the resin bonded sand properties. It is likely that difference in chemical composition and structural isomers between Thai and imported resins can give rise to dissimilar flow (viscosity), curing, and bond strength properties between resins and sand particles. Nevertheless, a more clearer picture of how different chemical composition, residual content, inorganic, metal and metal oxide influence resin and resin bonded sand properties has not been established. This obviously suggests a need of further investigation.

4.1.2.3.2 Differential Scanning Calorimeter (DSC)

The DSC thermogram of Thai resin and imported resin are given in the Appendices, Figure B-2. It can be seen that the DSC results show a board endothermic transition temperature in a range of $70\text{-}82^{\circ}$C for imported resin and of $82\text{-}88^{\circ}$C for Thai resin. The observed endothermic transition should represent softening (T_g) and melting (T_m) temperature range of the resin, where the relative wide range of transition can be

attributed to heterogeneous characteristics of the uncured novolac resins. The endothermic transition temperatures of imported resin are lower than those of Thai resin. This result also agree well with better flowability of the impored resin, as compared to Thai resin. As presented in Table 4.4, higher plate flow property (flow length) of imported resin ≈ 48 mm is an implication of softer resin. The stiffer Thai resin has a plate flow specification of ≈ 37mm.

4.1.2.3.3 Melting Point Measurement

This apparatus is useful for determining melting point of the resins. The measured melting point values of imported and Thai resin are 82°C and 91°C, respectively. This result again reveals a softer characteristic with better flow of imported resin, as compared with Thai resin. Overall observations may suggest that coating temperature (sand temperature) for imported resin can be set lower than the condition applied to Thai resin to obtain a more or less the same coating characteristics.

4.2 Characteristics of Bonded-Sand Studies by SEM

Resin-bonded sands are now widely used major molding media for both cores and molds. The mechanical properties of resin-bonded sands will depend upon the strengths and characteristics of the individual sand-resin joints. In practice, measurements of mechanical properties such as tensile, compressive, and bending strength are normally measured because these data infer the nature of the bond strength between resin and sand grains.

Visual examination of fracture surfaces by SEM can also contribute to an understanding of bonding and bond strengths. SEM examination gives perspective views of the sand surface, the sand-binder interface, and the fractured bonds. Such visual information may be useful in understanding mechanical strength measurements and other properties.

4.2.1 Characteristics of Resin-Bonded Sands

A comparison of bending strengths of resin coated sand has been made between the experimental and foundry processes. The mean experimental data with standard deviations are collected in Table 4.6. For raw data, this is given in the Appendices, Table A-1.

Table 4.6 The bending strength of resin coated sand from experimental and one foundry

processes

Resin used	Bending strength (kg/cm^2) from Experimental	Bending strength (kg/cm^2) from one foundry	Ratio (experimental / foundry)
1.7% FD-1 (Australian sand)	19.4 ± 2.4	20-30 (25)	0.78
2.1% FD-1 (Australian sand)	22.1 ± 3.0	28-34 (31)	0.71
2.4% FD-1 (Australian sand)	28.7 ± 3.4	30-38 (34)	0.84
3.2% FD-1 (Reclaimed sand)	36.9 ± 2.9	39-49 (44)	0.84
2.7% PSM-6412 (Rayong sand)	46.6 ± 4.6	48-58 (53)	0.87
4.3% PSM-6412 (Rayong sand)	64.7 ± 4.1	64-71 (67.5)	0.96

Note: ( ) is mean values.

From Table 4.6, it can be seen that the bending strength of resin coated sand from the experimental mixes are lower than those produced in the foundry. These differences can be explained by the fact that the foundry process has complete production mixing equipment including temperature controller system, cooling system, suitable impeller, air inlet system, air outlet suction system, etc. The experimental mixing unit was obviously

much less sophisticated in construction and had basic temperature control (thermometer), air pressure equipment, impeller, etc. The experimental mixing and coating techniques were expected to be less efficient than the foundry technique, but it was believed that consistent mixing would be obtained. The experiment values tend to confirm that this was the case, since the experimental results had similar spread to those from the foundry. The results in Table 4.6 show that the bending strength increases with increasing resin content. It can be noticed that at high resin content there is little difference between the experimental and production foundry mixes. At lower resin content, the strength ratio of experimental/foundry mixes is lower. This suggests that lower resin content mixes are more sensitive to mixing conditions.

Fracture surfaces of resin-bonded sands were examined using the SEM after the specimens were lightly gold coated. SEM micrographs of bend fracture surface are shown in Figure 4.9-4.14. These have been used to study the resin bonds (bridges) between the sand grains.

Huang and Mobley (1986) suggest that a number of qualitative or semi-quantitative relations have been reported on the bonding mechanism in clay-water or resin-bonded sands. Bonding mechanism is used herein to relate the macro- and microscopic features and mechanisms which occur and lead to the adherence between the components and the resultant characteristic strengths of the resin-bonded sands. The strength of resin-bonded sands depends on the two principle factors: a) the strength of the individual resin-sand joints, and b) the contact area of the resin-sand joint which participates in the load carrying and fracture process, as shown in Figure 4.15.

Figure 4.9 SEM micrographs of fractured surfaces (100x) and a bridge of sand grains (500x) of 1.7% FD-1 (Australian sand)

Figure 4.10 SEM micrographs of fractured surfaces (100x) and a bridge of sand grains

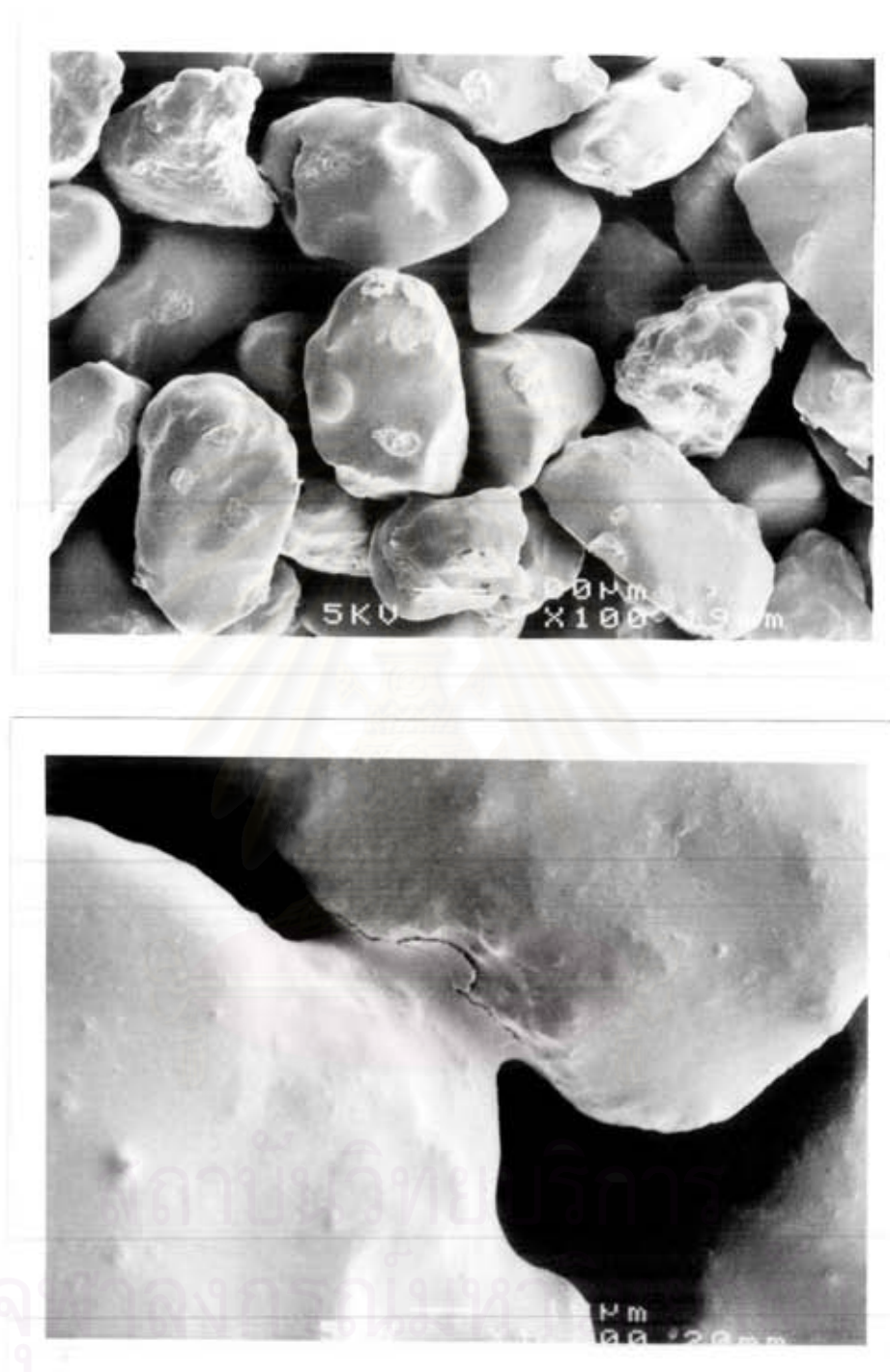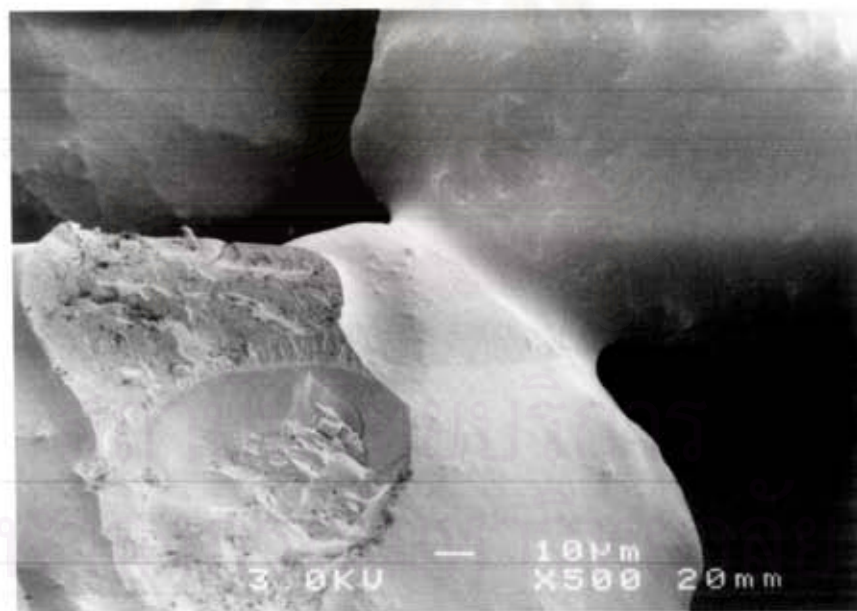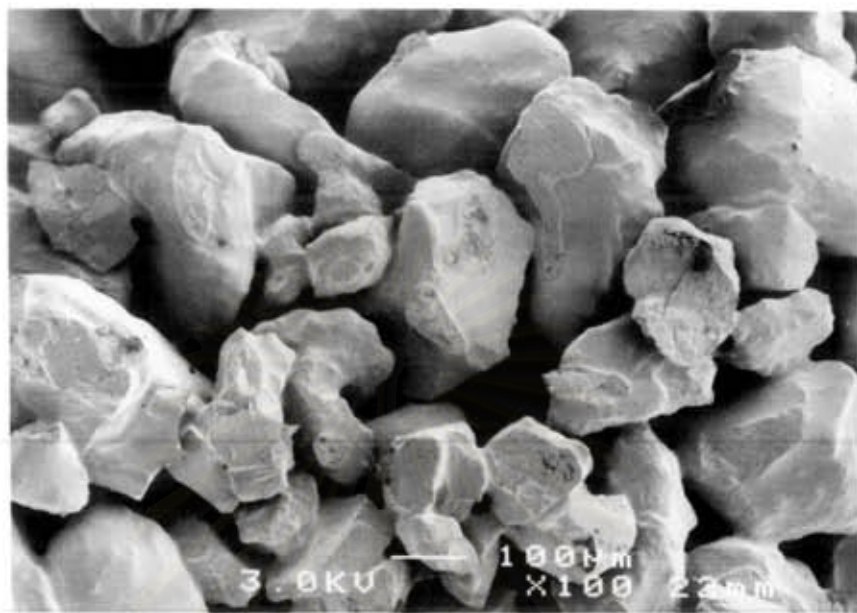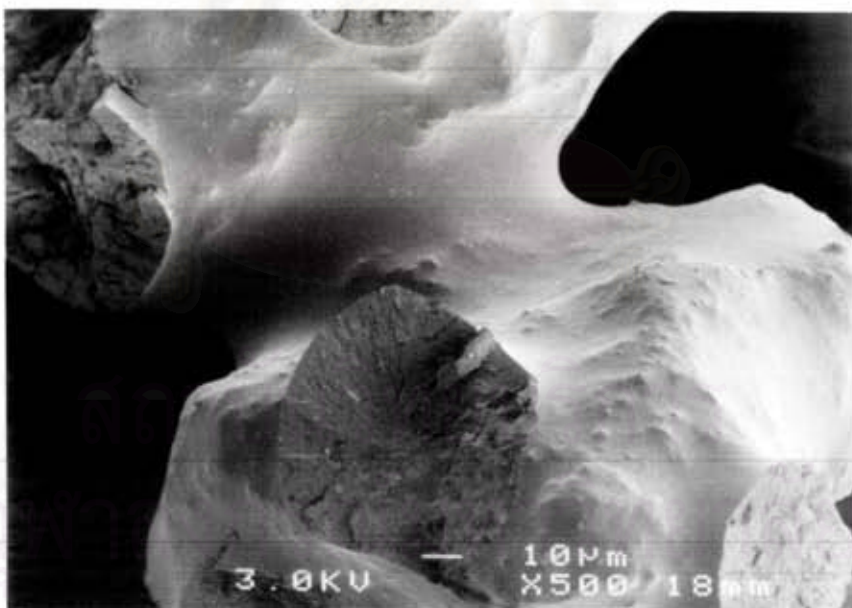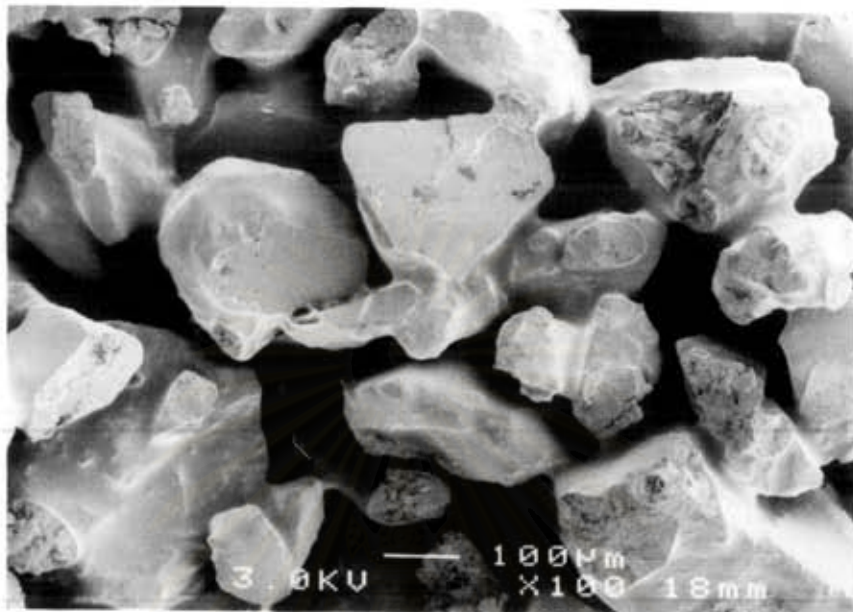(500x) of 2.1% FD-1 (Australian sand)

Figure 4.11 SEM micrographs of fractured surfaces (100x) and a bridge of sand grains
(500x) of 2.4% FD-1 (Australian sand)

Figure 4.12 SEM micrographs of fractured surfaces (100x) and a bridge of sand grains
(500x) of 3.2% FD-1 (reclaimed sand)

Figure 4.13 SEM micrographs of fractured surfaces (100x) and a bridge of sand grains
(500x) of 2.7% PSM-6412 (Rayong sand)

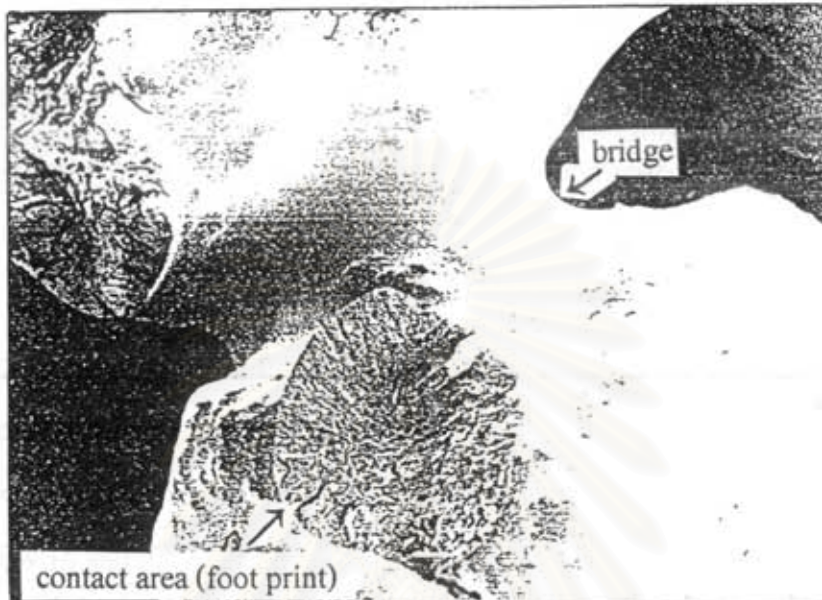Figure 4.14 SEM micrographs of fractured surfaces (100x) and a bridge of sand grains

(500x) of 4.3% PSM-6412 (Rayong sand)

Figure 4.15 Show the bridge and contact area of resin-bonded sands

Figure 4.9 shows SEM micrographs of fracture surfaces of 1.7% FD-1. The specimen was examined with a magnification of 100 times (100x). The sand grains are intact and there is no sign of fracture of sand particles. The bonds which appear to have small footprints at points of contact have separated at the sand grain surfaces as seen in the view at 500x.

Figure 4.10-4.12 show SEM micrographs of fracture surfaces of 2.1%, 2.4%, and 3.2% FD-1, respectively. The magnification is 100x and 500x. For micrographs of 2.1% and 2.4% FD-1, there were no obvious differences.

Figure 4.13 and 4.14 illustrate micrographs of fracture surface of 2.7% and 4.3% PSM-6412, respectively. The magnification is also 100x and 500x. Resin necks or bridges, which connect adjoining sand particles can be cleanly seen in these pictures. In Figure 4.12, it shows that the contact areas (footprints) are smaller than that of resin 4.3% PSM 6412, seen in Figure 4.13. The higher magnification (500x) clearly shows the bonding bridge. Based on these observation, the big footprint can occur with increasing the amount of added binder.

These micrographs can be further explained by quantitative analysis in order to understand the bending strength values. These quantitative measures can be determined by calculation of contact area on sand grains. The resulting values are shown in Table 4.7 and plotted in Figure 4.16 and 4.17. For raw data is given in Appendices, Table A-6.

From Table 4.7, it was found that the bending strengths increase with increasing contact area of the resin-sand joints. The contact area also relates to bridge length. As the contact area of resin-sand joint increases, the measured bridge diameter of such bonds (shown an increment). Higher bending strength of imported resin-bonded sand samples as compared to those of Thai resin bonded samples relates well larger contact areas and longer bridge diameter of the joints.

Figure 4.16 shows that bending strengths of resin-bonded sand specimens increase with increasing contact area. The trend revealed that imported resin is higher bending strength and contact area than Thai resin. The contact area also increases with increasing amount of resin, as shown in Figure 4.17. The bending strength and contact area of Thai resin-coated sand are lower than that of imported resin coated sand. These

results can be mainly attributed to different structural isomers and molecular weight of Thai and imported resins which directly influence flow property, viscosity, cure rate or gelation time of the resins. These variables have great influence on the reaction between resin and hexamine (crosslinking) as well as resin-bonded sand (bending strength). The highest strength value is obtained with resins of low melt and low viscosity (high flow) as imported resin of all these resin-bonded sand specimens. Other possible factors affecting bending strength of the resin-bonded sand sample may involve hexamine content. Hexamine content used with imported and Thai resins in this study are 15% and 17% by weight of resin, respectively. As reported in literature, it is increasing to note further gain in strength property (especially hot strength) appear above 15% hexamine. However, a better understanding of a role of the hexamine content requires a further study.

Table 4.7 The relation of the bending strength, contact area and bridge diameter of various resins used

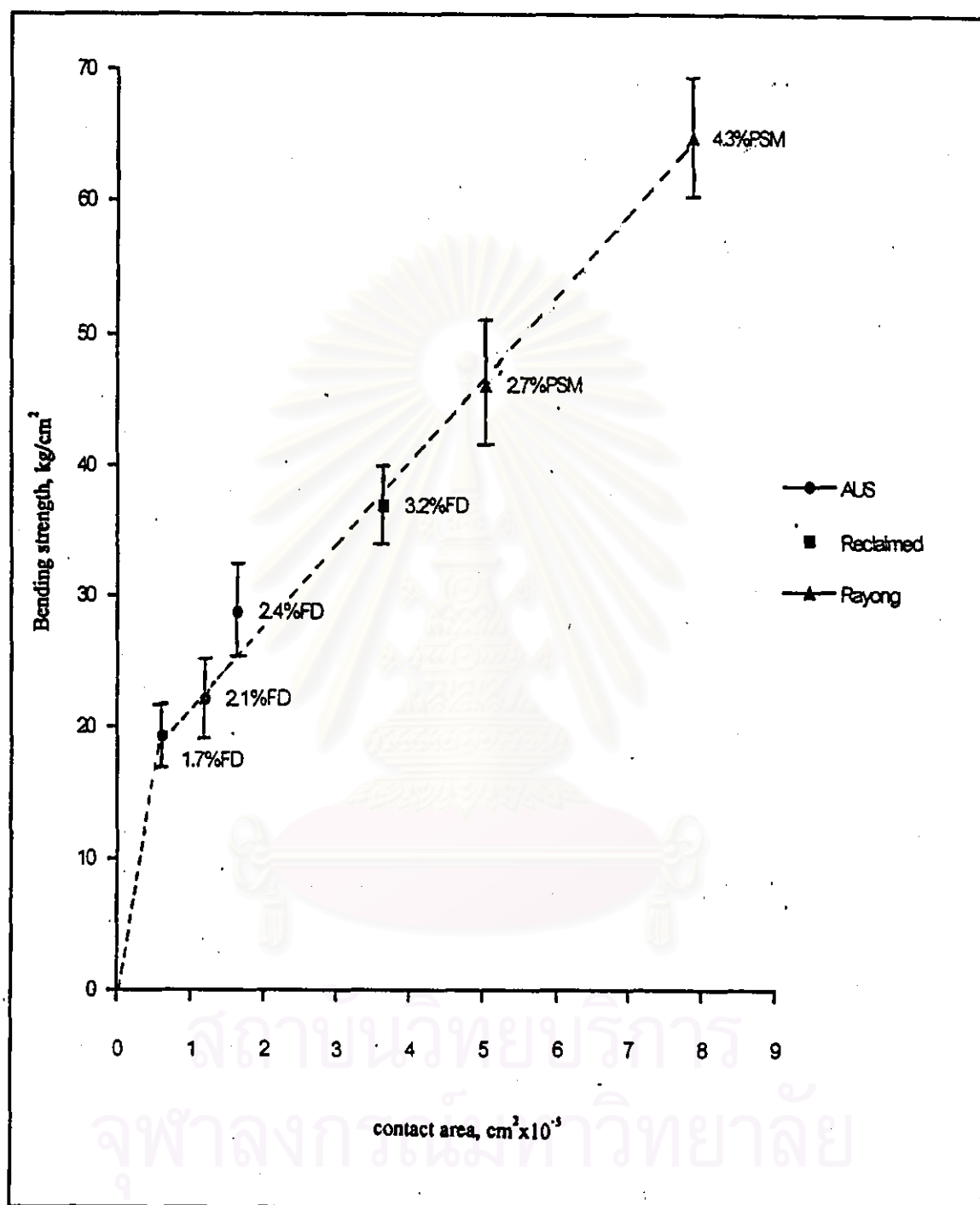| Resin used	Bending strength (kg/cm^2) from Experimental	Contact area (cm^{2}x 10^{-5})	Bridge diameter, μm
1.7% FD-1 (Australian sand)	19.4 $\pm$ 2.4	0.6 $\pm$ 0.3	28 $\pm$ 5
2.1% FD-1 (Australian sand)	22.1 $\pm$ 3.0	1.2 $\pm$ 0.5	39 $\pm$ 7
2.4% FD-1 (Australian sand)	28.7 $\pm$ 3.4	1.7 $\pm$ 0.2	46 $\pm$ 2
3.2% FD-1 (Reclaimed sand)	36.9 $\pm$ 2.9	3.5 $\pm$ 1.1	66 $\pm$ 12
2.7% PSM-6412 (Rayong sand)	46.6 $\pm$ 4.6	5.1 $\pm$ 1.4	80 $\pm$ 17
4.3% PSM-6412 (Rayong sand)	64.7 $\pm$ 4.1	7.9 $\pm$ 1.1	100 $\pm$ 10

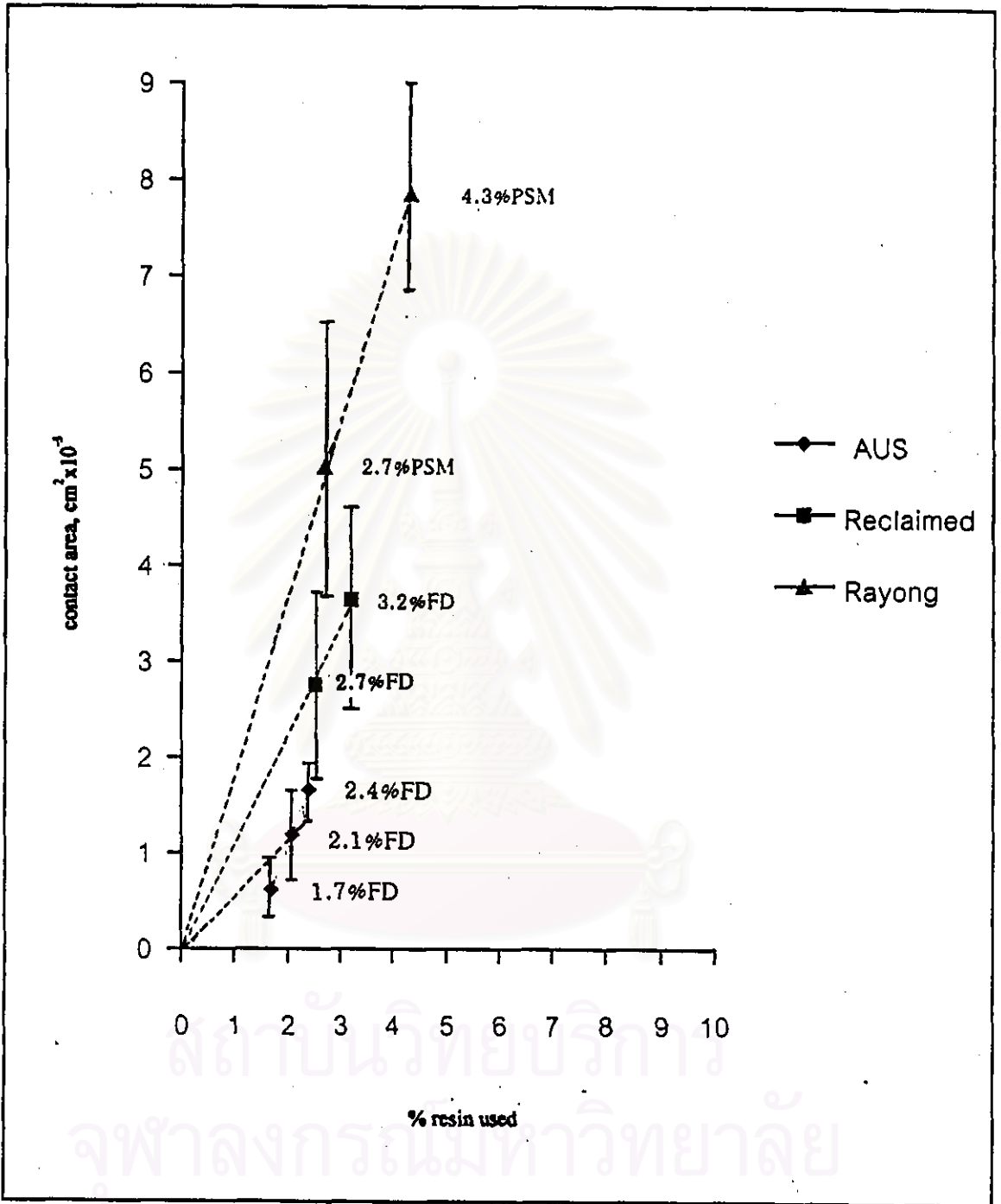**Figure 4.16** The bending strength and contact area of resin-bonded sands of various resins used

Figure 4.17 The relation of various resins used and contact area of resin-bonded sand

4.2.2 Characteristics of Resin Coated Sand Using Resin Blends of Thai and imported Resins (PSM-FD)

Imported resin (approximately twice the price of Thai resin) is more expensive than Thai resin but costs of resin in sand mixes may be reduced by blending of the Thai with imported resins. Some experiments were therefore performed in blends of the two resins (PSM-FD) based on total resin additions of 2.7 and 4.3 % by weight in sand mixes. Both Rayong sand and reclaimed sand have been used in these tests.

Experimental results are given in the Appendices, Table A-2 to A-5. The mean experimental data with standard deviations are also collected in Table 4.8-4.11. These values are plotted in Figure 4.18.

Table 4.8 The properties of resin blends (PSM-FD) coated sand with various Thai resin by weight percent (standard formula of 2.7% PSM-6412 with Rayong sand)

Thai resin added, by weight percent	Bending strength, (kg/cm^2)	Stick point, $^\circ C$	AFS Fineness number
0	46.6 ± 4.6	84.3 ± 0.6	52.0 ± 0.4
20	38.9 ± 3.2	91.3 ± 0.6	52.5 ± 0.8
40	31.3 ± 3.0	92.8 ± 0.8	52.8 ± 0.2
60	24.3 ± 2.2	93.0 ± 1.0	51.3 ± 0.7
80	23.6 ± 1.8	95.5 ± 0.5	51.3 ± 1.2
100	20.6 ± 2.4	99.0 ± 3.0	51.3 ± 0.7

Table 4.9 The properties of resin blends (PSM-FD) coated sand with various Thai resin by weight percent (standard formula of 2.7% PSM-6412 with reclaimed sand)

Thai resin added, by weight percent	Bending strength, (kg/cm^2)	Stick point, $^\circ C$	AFS Fineness number
0	61.4 ± 5.3	86.5 ± 0.5	49.9 ± 0.2
20	55.2 ± 3.8	87.7 ± 0.6	49.5 ± 0.5
40	46.4 ± 2.8	89.8 ± 1.1	49.4 ± 0.8
60	35.5 ± 2.1	90.8 ± 0.8	49.6 ± 0.6
80	27.0 ± 1.6	93.6 ± 0.6	49.6 ± 0.7
100	25.5 ± 3.1	99.3 ± 1.5	48.4 ± 0.5

Table 4.10 The properties of resin blends (PSM-FD) coated sand with various Thai resin

by weight percent (standard formula of 4.3% PSM-6412 with Rayong sand)

Thai resin added by weight percent	Bending strength, (kg/cm^2)	Stick point, ^{o}C	AFS Fineness number
0	64.4 ± 6.9	83.3 ± 0.6	50.8 ± 0.7
20	58.0 ± 3.9	85.7 ± 0.6	50.3 ± 0.7
40	48.9 ± 4.6	87.3 ± 0.6	49.5 ± 0.5
60	42.5 ± 3.4	91.7 ± 0.6	51.5 ± 0.5
80	40.8 ± 2.5	94.7 ± 0.6	50.5 ± 0.5
100	33.8 ± 4.1	100.7 ± 1.5	51.0 ± 1.0

Table 4.11 The properties of resin blends (PSM-FD) coated sand with various Thai resin

by weight percent (standard formula of 4.3% PSM-6412 with reclaimed sand)

Thai resin added by weight percent	Bending strength, (kg/cm^2)	Stick point, ^{o}C	AFS Fineness number
0	73.4 ± 3.0	83.0 ± 1.0	49.1 ± 0.9
20	65.7 ± 4.5	85.1 ± 0.2	50.2 ± 0.8
40	59.7 ± 5.4	86.3 ± 0.6	49.0 ± 1.0
60	54.0 ± 4.7	90.8 ± 0.8	50.2 ± 1.0
80	49.3 ± 3.8	97.2 ± 0.8	49.5 ± 0.5
100	41.4 ± 4.3	98.7 ± 0.6	50.0 ± 0.5

From Table 4.8-4.11, it was found that the bending strength decrease with increasing Thai resin content. The stick points increase as Thai resin content increases. This can be a result of normally higher melting point of Thai resin. The AFS fineness number values show that each sand mixing was consistent in grain size and distribution enabling confident comparisons between the various resin blends.

Experimental results show clearly that the bending strength decrease with Thai resin addition, as seen in Figure 4.18. Since, the overall flow, thermal and molecular weight properties of Thai resin have influenced to formation of chemical bonding in resin-bonded sands. It gives a decrease in bending strength as % Thai resin content is added. Fracture surfaces of resin-bonded sands were also examined by the SEM, as illustrated in Figure 4.19-4.24.

Figure 4.19-4.24 show SEM micrographs of fracture surfaces of 0, 20, 40, 60, 80, 100 Thai resin by weight percent in resin blends coated sand. They have difference in contact area and bridge length, as shown in Table 4.12. For raw data is given in the Appendices, Table A-7.
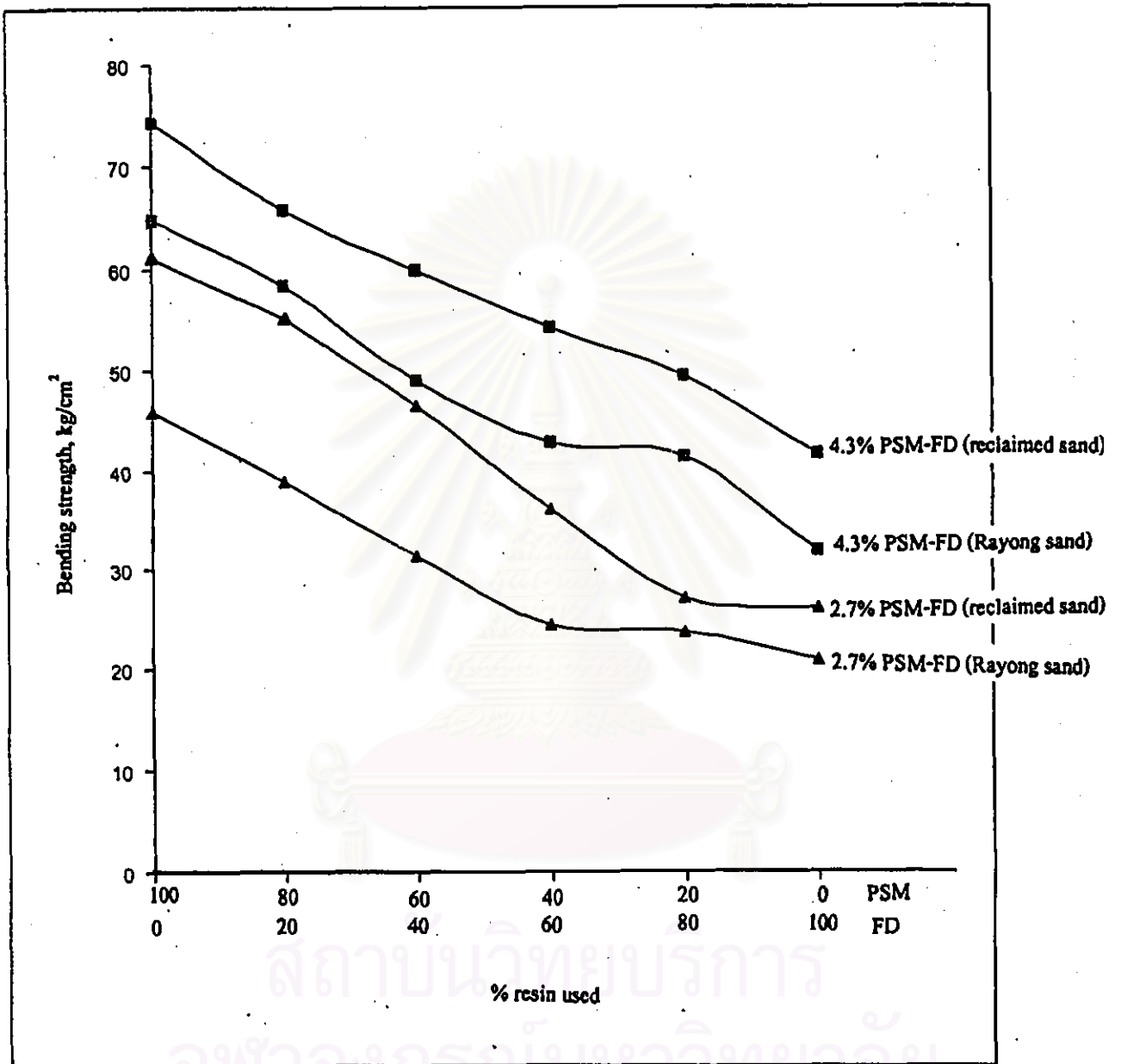
Figure 4.18 Influence of amount of Thai resin added in resin blends (PSM-FD) with bending strength
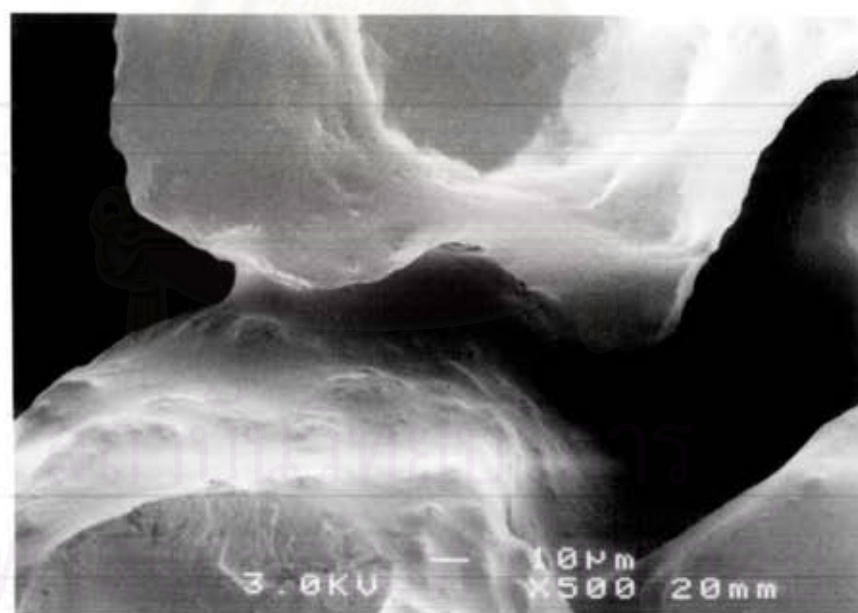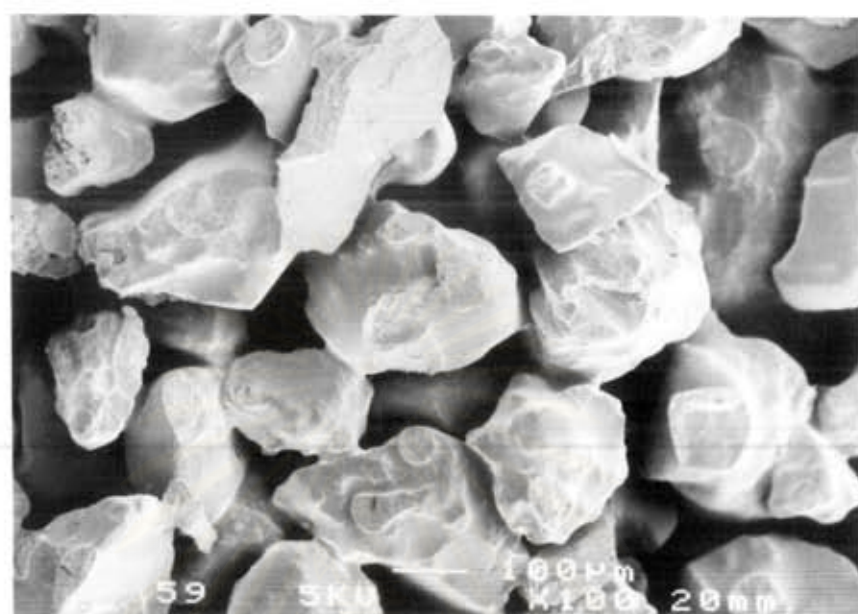
Figure 4.19 SEM micrographs of fractured surface (100x) and a bridge of sand grains
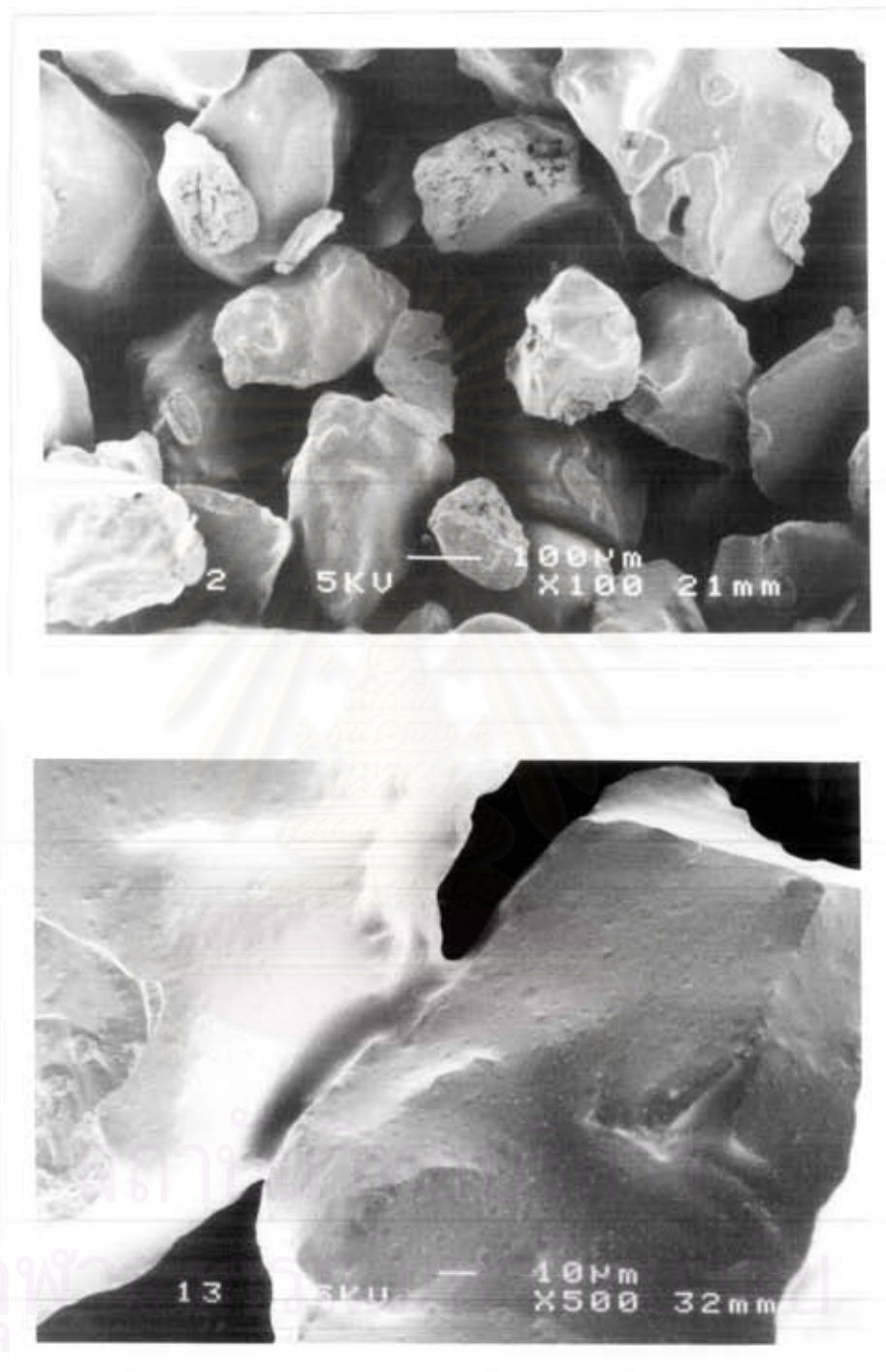(500x) of standard formula 2.7% PSM (0% FD) with reclaimed sand

Figure 4.20 SEM of micrographs fractured surface (100x) and a bridge of sand grains
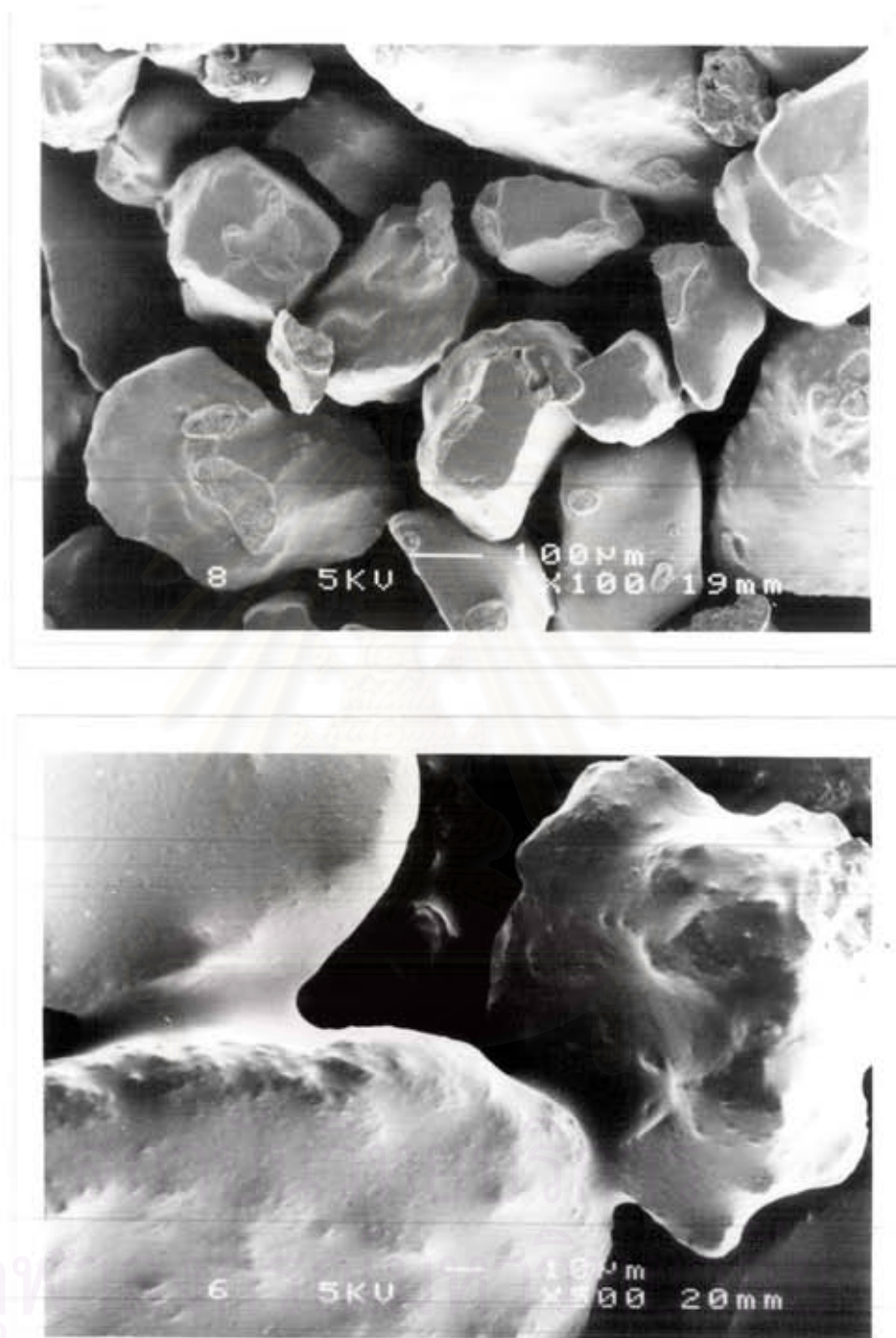(500x) of 2.7% PSM-FD using 20% Thai resin (by weight percent)

Figure 4.21 SEM micrographs of fractured surface (100x) and a bridge of sand grains
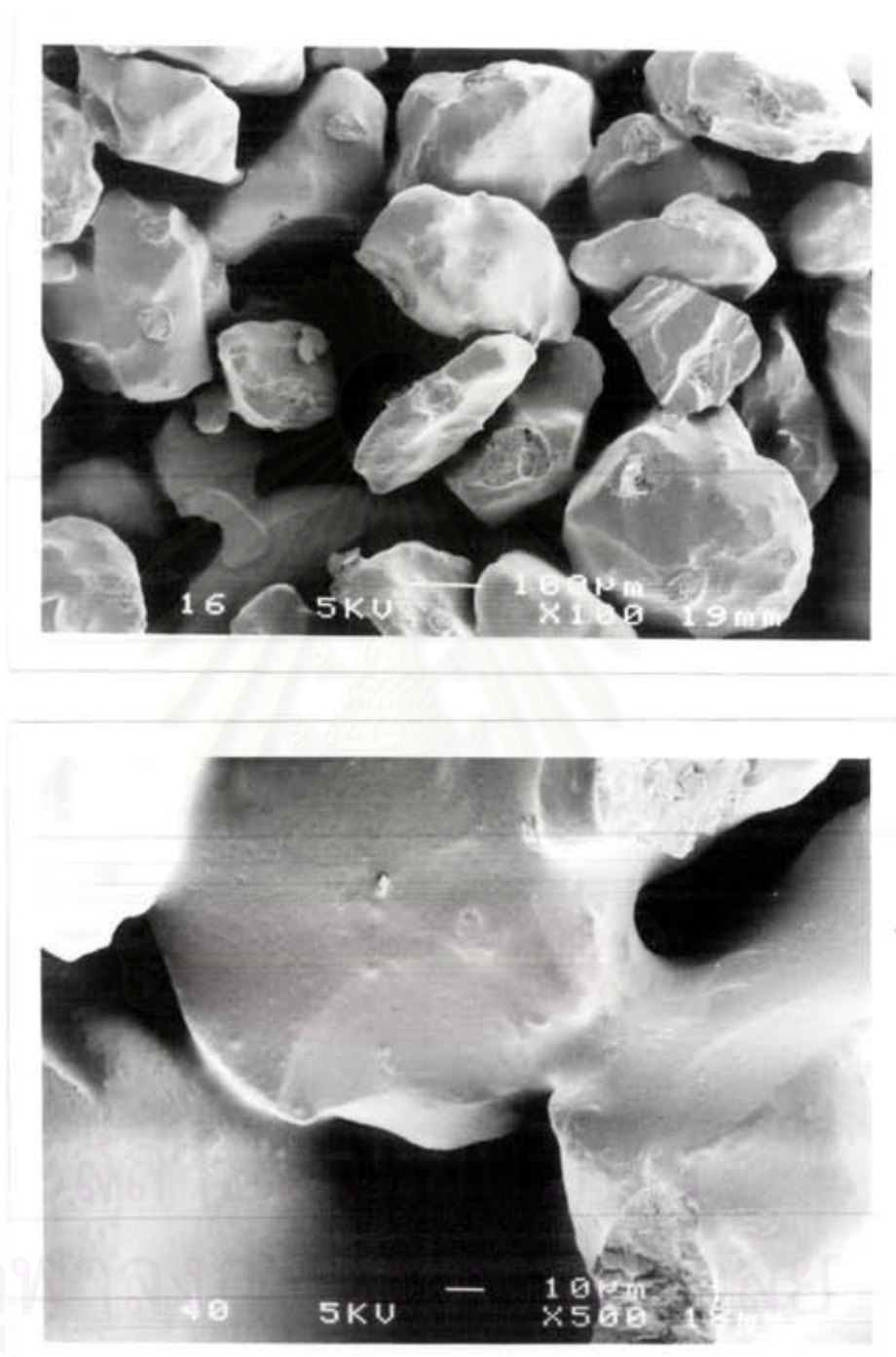(500x) of 2.7% PSM-FD using 40% Thai resin (by weight percent)

Figure 4.22 SEM micrographs of fractured surface (100x) and a bridge of sand grains
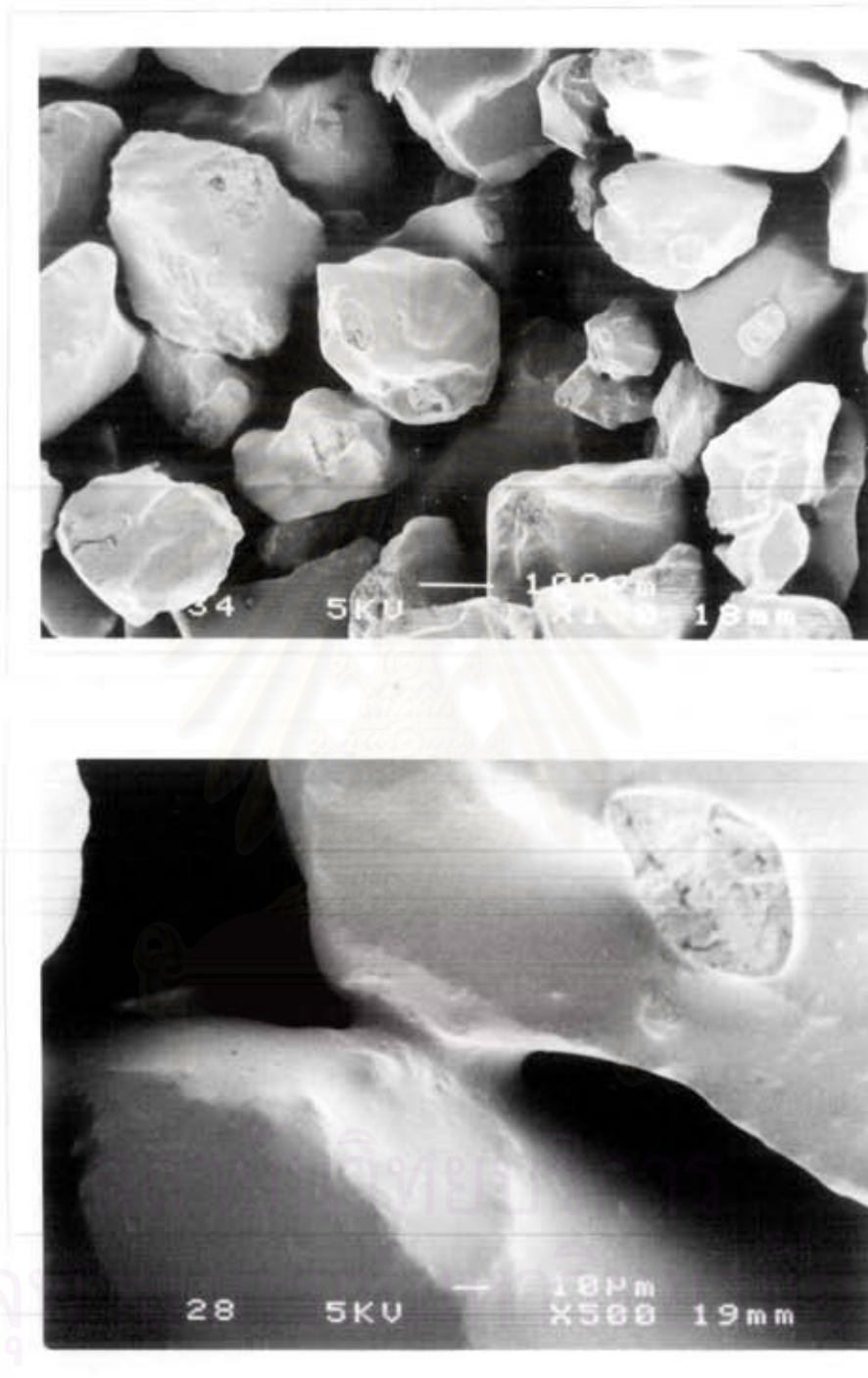(500x) of 2.7% PSM-FD using 60% Thai resin (by weight percent)

Figure 4.23 SEM micrographs of fractured surface (100x) and a bridge of sand grains
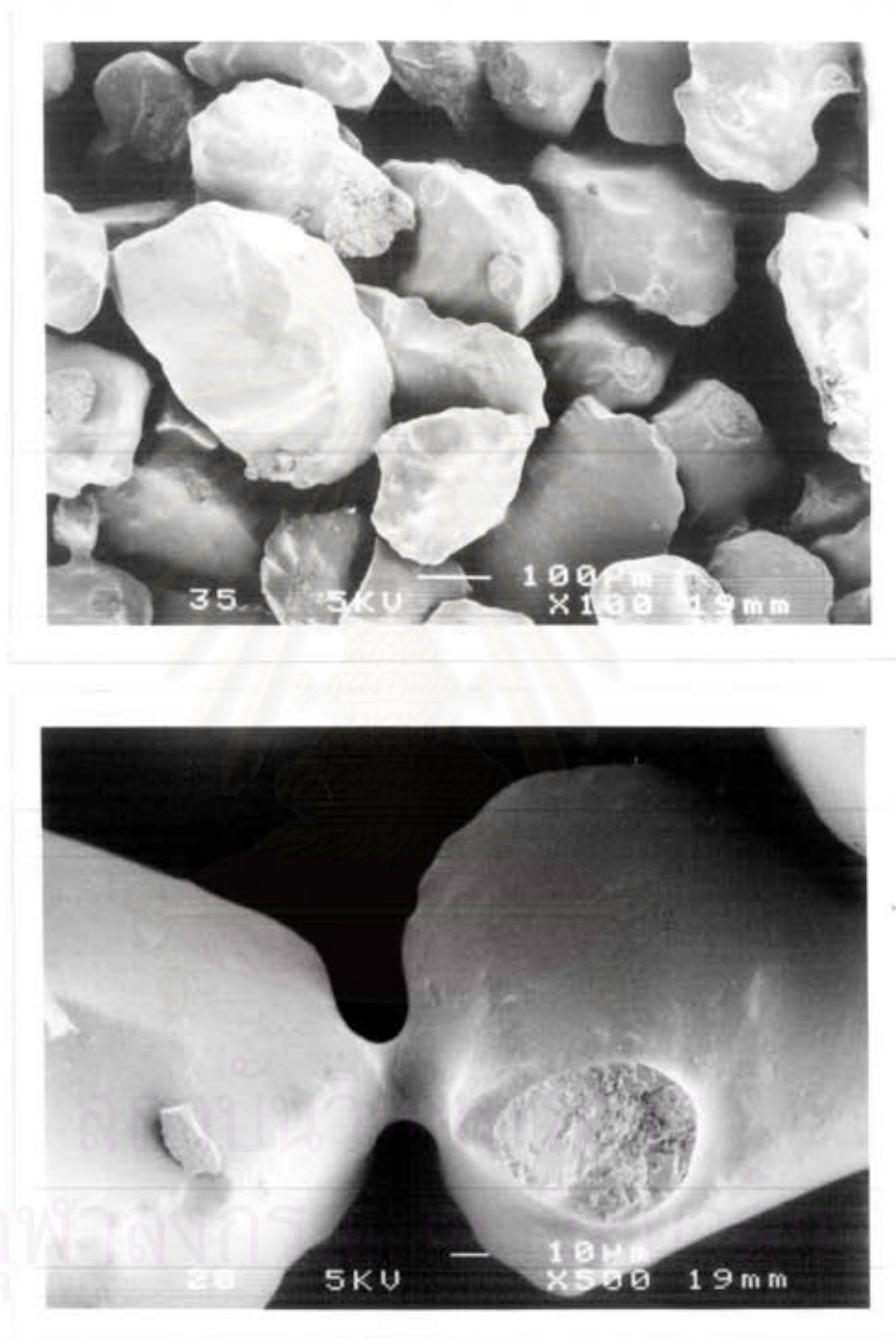(500x) of 2.7% PSM-FD using 80% Thai resin (by weight percent)

Figure 4.24 SEM micrographs of fractured surface (100x) and a bridge of sand grains
(500x) of 2.7% PSM-FD using 100% Thai resin (by weight percent)

The quantitative analysis of resin blends (PSM-FD) coated sand was also determined by calculation of contact area, as shown in Table 4.12. It was found that contact area and bridge diameter decrease with increasing amount of Thai resin addition. Thai resin properties have a tendency to harden before it has time to from a strong bond between sand grains because of its short flow length and fast gelation time. Thus, the properties of resin are very important using in coating sand. Such imported resin gives the good flowability, low melt viscosity, longer gelation time, as compared with Thai resin. These variables are obtained the best strength of resin-bonded sands.

Table 4.12 The relation of the bending strength, contact area and bridge diameter in resin blends (PSM-FD) coated sand (standard formula of 2.7% PSM with reclaimed sand)

Thai resin used by weight percent	Bending strength (kg/cm^2)	Contact area $(cm^2 x\ 10^{-5})$	Bridge diameter, μm
0	61.4 ± 5.3	6.4 ± 2.4	89 ± 18
20	55.2 ± 3.8	5.3 ± 1.6	81 ± 13
40	46.4 ± 2.8	4.9 ± 3.0	76 ± 12
60	35.5 ± 2.1	3.0 ± 1.4	61 ± 14
80	27.0 ± 1.7	2.8 ± 0.6	60 ± 6
100	25.5 ± 3.1	2.7 ± 1.1	58 ± 11

When difference type of sands are used, comparison of the bending strength is made and summarized in Table 4.8-4.11. It was found that the reclaimed sand gives higher bending strength than Rayong sand for the same resin addition, as illustrated in Figure

4.25. This reclaimed sand has a smaller particle and rounded shape because Australian sand was mixed with Rayong sand in reclamation process.

In the case of reclaimed sand, Thai resin content of 20% by weight percent gives the bending strength in a range of those obtain for the two specific formula (2.7% and 4.3% PSM-6412). In one foundry plant, the 2.7% PSM-6412 with reclaimed sand is normally used for Shell mold. Results of the experimental show that the desirable properties of resin coated sand can also be obtained using resin blends of 80/20 and 70/30 (imported to Thai resins). In this specific foundry plant, the 4.3% PSM-6412 formula is more often with Rayong sand rather than the reclaimed sand.

In summary, the possibility of using blends of Thai and imported resins was examined with a view to cost saving of based on the standard formula used in one foundry, 2.7% PSM (reclaimed sand), as illustrated in Figure 4.26. It was found that the resin blends of 80/20 and 70/30 imported and Thai resins show desirable bending strength of resin coated sand. Experimental results demonstrate a possible cost saving of up to 30% of imported resin in Shell mold production by effective use of resin blends as the binder in resin coated sand.
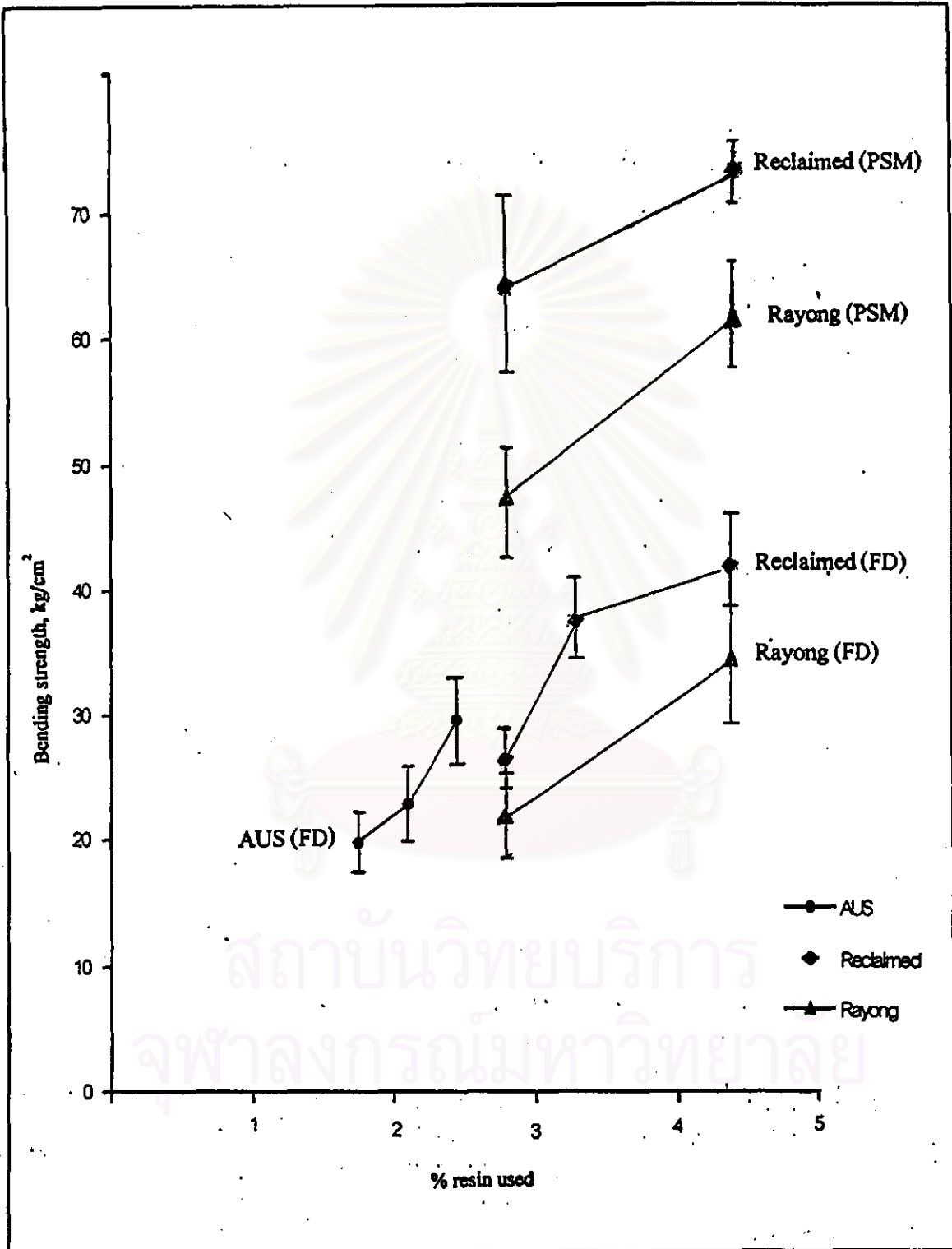
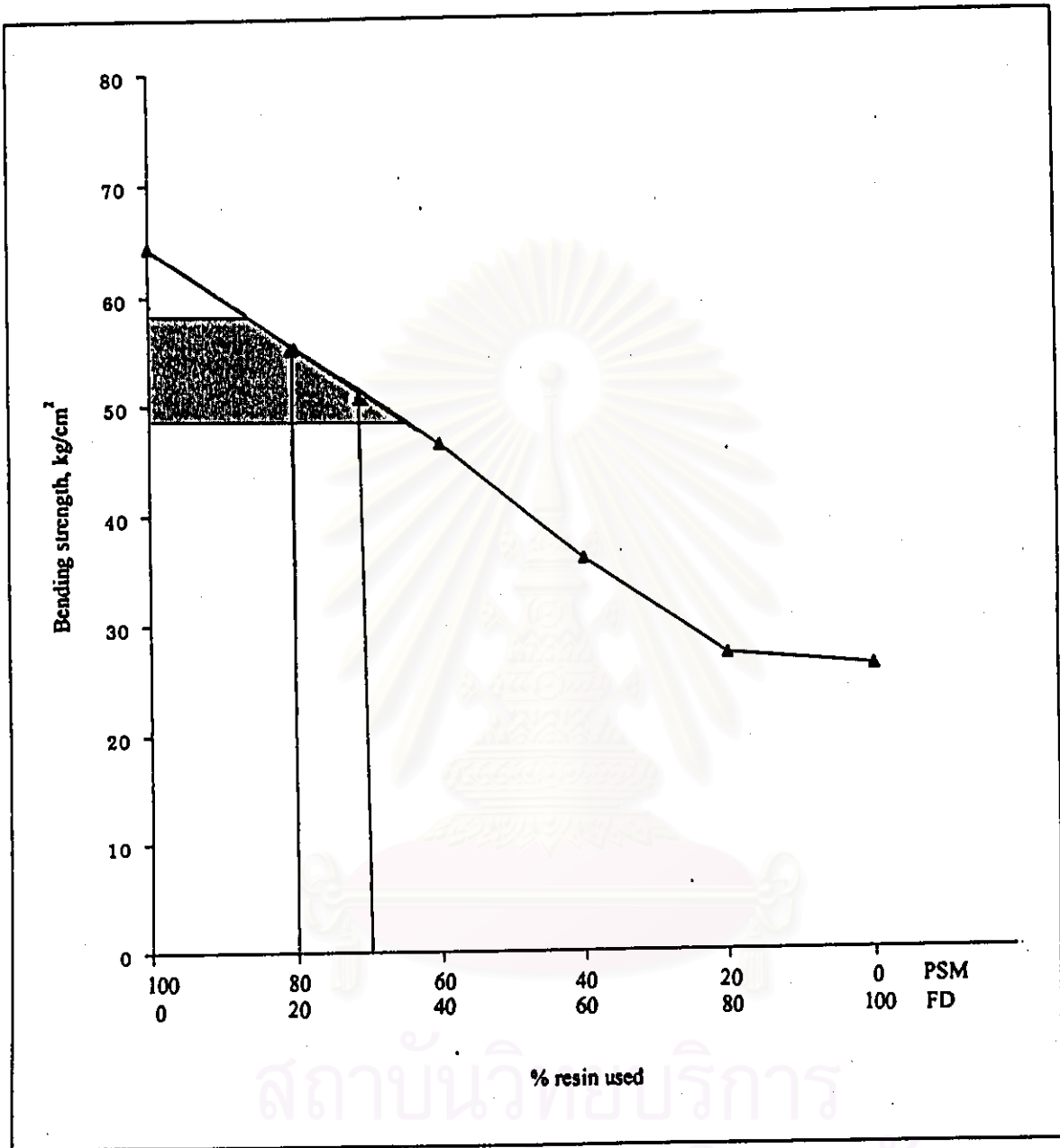Figure 4.25 The influence of types of sand with bending strength

Figure 4.26 The bending strength of resin blends (PSM-FD) coated sand in 80/20 and 70/30 imported resin to Thai resin in desirable values for used in shell production (average bending strength of specific formula $\approx$ 48-58 kg/cm^2) is shown in shaded area.